Convexification Numerical Method for a Coefficient Inverse Problem for the Riemannian Radiative Transfer Equation *

Michael V. Klibanov †, Jingzhi Li ‡, Loc H. Nguyen †, Vladimir G. Romanov §, and Zhipeng Yang ¶

Abstract. The first globally convergent numerical method for a Coefficient Inverse Problem (CIP) for the Riemannian Radiative Transfer Equation (RRTE) is constructed. This is a version of the so-called "convexification" method, which has been pursued by this research group for a number of years for some other CIPs for PDEs. Those PDEs are significantly different from the RRTE. The presence of the Carleman Weight Function (CWF) in the numerical scheme is the key element which insures the global convergence. Convergence analysis is presented along with the results of numerical experiments, which confirm the theory. RRTE governs the propagation of photons in the diffuse medium in the case when they propagate along geodesic lines between their collisions. Geodesic lines are generated by the spatially variable dielectric constant of the medium.

Key words. geodesic lines, Riemannian metric, Carleman estimate, coefficient inverse problem, global convergence, convexification, numerical studies

MSC codes. 35R30, 65M32

1. Introduction. The conventional steady state radiative transfer equation (RTE) governs light propagation in the diffuse medium, such as, e.g. turbulent atmosphere and biological media [22]. Inverse problems for the RTE have applications in, e.g. problems of seeing through a turbulent atmosphere and in an early medical diagnostics. In the latter case the near infrared light with a relatively small energy of photons is used, see, e.g. [5]. However, it is assumed in the RTE that photons propagate along straight lines between their collisions. On the other hand, since the dielectric constants in heterogeneous media, such as, e.g. ones mentioned above, vary in space, then photons actually propagate along geodesic lines between their collisions. These lines are generated by the Riemannian metric $\sqrt{\varepsilon_r(\mathbf{x})}\,|d\mathbf{x}|$. Here and below $\mathbf{x} = (x, y, z) \in \mathbb{R}^3$ and $\varepsilon_r(\mathbf{x})$ is the spatially distributed dielectric constant, so that

$n(\mathbf{x}) = \sqrt{\varepsilon_r(\mathbf{x})}$ is the refractive index. To take this into account, the so-called Riemannian Radiative Transfer Equation (RRTE) should be used.

This is the first publication, in which a globally convergent numerical method, the so-called convexification method, is constructed for a Coefficient Inverse Problem (CIP) for the steady state RRTE. In the past, numerical methods for inverse problems for the steady state RTE were mostly developed for the case of inverse source problems [13, 14, 47]. Inverse source problems are linear. On the other hand, CIPs are nonlinear. We refer to two recent publications of this research team [34, 35] for two versions of the convexification numerical method for a CIP for the RTE. The presence of the Riemannian aspect in the RRTE causes significant additional difficulties for the corresponding CIP, as compared with the case of the RTE in [34, 35]. The authors are unaware about other numerical methods for CIPs neither for the RTE nor for the RRTE.

Various uniqueness and stability results for inverse problems for both RTE and RRTE, including quite general forms of the latter equation, were published in the past. Since this paper is concerned only with a numerical method, then we refer now only to a limited number of such publications [3, 4, 5, 17, 27, 36, 38, 41].

The phenomena of ill-posedness and nonlinearity of CIPs are well known and cause serious challenges for their numerical solutions. Both a powerful and popular concept of numerical methods for CIPs is based on the minimization of appropriate least squares cost functionals, see, e.g. [1, 7, 6, 18, 19, 16, 21] and references cited therein. Since such a cost functional is typically non convex, then it usually suffers from the phenomenon of local minima and ravines, see, e.g. [46], i.e. the availability of a good first guess about the true solution is a necessary assumption of the convergence analysis of these numerical methods.

Remark 1.1. *We call a numerical method for a CIP globally convergent if a theorem is proven, which claims that this method delivers at least one point in a sufficiently small neighborhood of the true solution without any advanced knowledge of this neighborhood. The size of that neighborhood should depend only on the level of noise in the data.*

The key element of our numerical method is the presence of a Carleman Weight Function (CWF) in a certain weighted least squares cost functional. This presence ensures the global strict convexity of that functional. This is why we call our method "convexification". The CWF is the function, which is involved as the weight function in the Carleman estimate for the corresponding PDE operator. Our convergence analysis ensures the global convergence of the gradient descent method of the minimization of that functional to the true solution of our CIP, as long as the level of the noise in the data tends to zero. The apparatus of the Riemannian geometry is also used here. Results of numerical experiments are presented, and they confirm our theory.

The convexification concept generates globally convergent numerical methods since these methods do not rely on good first guesses about the solutions. The convexification was originally proposed in purely theoretical works [32, 29]. Its active numerical studies have started in 2017 after the publication [2], which has removed some obstacles for numerical implementations. In this regard, we refer to, e.g. [26, 33, 34, 35] and references cited therein.

Another important new element of this paper is Theorem 1 (section 3), which claims existence, uniqueness and positivity of the solution of for the forward problem for the RRTE.

An analog of this theorem for the non-Riemannian case was proven in [34]. The proof of Theorem 1 is constructive since it ends up with an analysis of a linear integral equation of the Volterra type. This equation is quite helpful in our numerical studies in section 6, since we solve it numerically to computationally simulate the data for the inverse problem. It is well known that such computational simulations form an important part of numerical studies of any inverse problem. The presence of the Riemannian aspect creates a significant additional difficulty in the proof of Theorem 1, as compared with the case of RTE in [34]. This difficulty is due to the necessity of working with the differential geometry, which, however, was not necessary to do in [34].

As to the apparatus of Carleman estimates, it was introduced in the field of CIPs in the publication [10], initially with the single goal of proofs of uniqueness theorems. Since then the idea of [10] was explored in many other publications, see, e.g. [8, 11, 12, 17, 23, 28, 30, 33, 38, 50] and references cited therein. The convexification principle represents an extension of the idea of [10] to the topic of globally convergent numerical methods for CIPs. Those numerical methods might be generalized and employed for important applications like, e.g. cloaking and quantum scattering studied in [40, 39].

We consider below only real valued functions. For the sake of definiteness, we work below in our theoretical derivations only with the 3d case. On the other hand, we present numerical results in the 2d case since the theory for the 2d case is completely similar with the one in the 3d case. In section 2 we pose both the forward and inverse problems for RRTE. In section 3 we formulate and prove the above mentioned Theorem 1. In section 4 we derive a version of the convexification method for our CIP. In section 5 we provide convergence analysis. Section 6 is devoted to numerical studies, which confirm our theory.

2. Statements of Forward and Inverse Problems. Let numbers $A, a, b, d > 0$, where

$$(2.1) \qquad 0 < a < b.$$

Define the rectangular prism $\Omega \subset \mathbb{R}^3$ and parts $\partial_1\Omega, \partial_2\Omega, \partial_3\Omega$ of its boundary $\partial\Omega$, as well as the line Γ_d where the external sources are:

$$(2.2) \qquad \begin{aligned} \Omega &= \{\mathbf{x} : -A < x, y < A, a < z < b\}, \\ \partial_1\Omega &= \{\mathbf{x} : -A < x, y < A, z = a\}, \ \partial_2\Omega = \{\mathbf{x} : -A < x, y < A, z = b\}, \\ \partial_3\Omega &= \{x = \pm A, y \in (-A.A), z \in (a, b)\} \cup \\ &\cup \{y = \pm A, x \in (-A, A), z \in (a, b)\}, \\ \Gamma_d &= \{\mathbf{x}_\alpha = (\alpha, 0, 0) : \alpha \in [-d, d]\}. \end{aligned}$$

Hence, Γ_d is a part of the $x-$axis. By (2.1) and (2.2) $\Gamma_d \cap \overline{\Omega} = \varnothing$.

Let the points of external sources $\mathbf{x}_\alpha \in \Gamma_d$. Let $\epsilon > 0$ be a sufficiently small number. To avoid dealing with singularities, we model the $\delta(\mathbf{x})-$function as:

$$(2.3) \qquad f(\mathbf{x}) = C_\epsilon \begin{cases} \exp\left(\frac{|\mathbf{x}|^2}{\epsilon^2 - |\mathbf{x}|^2}\right), & |\mathbf{x}| < \epsilon, \\ 0, & |\mathbf{x}| \geq \epsilon, \end{cases}$$

where the constant C_ϵ is such that

$$(2.4) \qquad C_\epsilon \int_{|\mathbf{x}|<\epsilon} \exp\left(\frac{|\mathbf{x}|^2}{\epsilon^2 - |\mathbf{x}|^2}\right) d\mathbf{x} = 1.$$

Hence, the function $f(\mathbf{x} - \mathbf{x}_\alpha) = f(x - \alpha, y, z) \in C^\infty(\mathbb{R}^3)$ plays the role of the source function for the point source $\{\mathbf{x}_\alpha\}$. We choose ϵ so small that

$$(2.5) \qquad f(\mathbf{x} - \mathbf{x}_\alpha) = 0, \quad \forall \mathbf{x} \in \overline{\Omega}, \quad \forall \mathbf{x}_\alpha \in \Gamma_d.$$

Let $\Gamma(\mathbf{x}, \mathbf{x}_0)$ be the geodesic line generated by the Riemannian metric $\sqrt{\varepsilon_r(\mathbf{x})}\,|d\mathbf{x}|$ and connecting the source $\mathbf{x}_0 \in \mathbb{R}^3$ with an arbitrary point $\mathbf{x} \in \mathbb{R}^3$,

$$(2.6) \qquad \Gamma(\mathbf{x}, \mathbf{x}_0) = \mathrm{argmin} \left\{ \begin{array}{l} \int_\gamma \sqrt{\varepsilon_r(\boldsymbol{\xi}(t))}\,dt, \ \text{where} \ \gamma(t) : [0,1] \to \mathbb{R}^3 \\ \text{is a smooth map with} \ \gamma(0) = \mathbf{x}_0, \ \gamma(0) = \mathbf{x}. \end{array} \right\}$$

Here $\varepsilon_r(\mathbf{x})$ is the spatially distributed dielectric constant of the medium, $1/\sqrt{\varepsilon_r(\mathbf{x})}$ is the dimensionless speed of light. We assume that the function $\varepsilon_r(\mathbf{x})$ satisfies the following conditions:

$$(2.7) \qquad \varepsilon_r(\mathbf{x}) \in C^3(\mathbb{R}^3),$$

$$(2.8) \qquad \varepsilon_r(\mathbf{x}) = 1, \quad \mathbf{x} \in \{\mathbf{x} \in \mathbb{R}^3 | \ |x| \geq A, |y| \geq A\} \cup \{\mathbf{x} \in \mathbb{R}^3 | \ z \leq a\},$$

$$(2.9) \qquad \partial_z \varepsilon_r(\mathbf{x}) \geq 0, \quad \mathbf{x} \in \mathbb{R}^3.$$

Let $\tau(\mathbf{x}, \mathbf{x}_0)$ be the first time of arrival at the point $\mathbf{x}$ of light generated at the point $\mathbf{x}_0$. Then [44, Chapter 3]

$$(2.10) \qquad \tau(\mathbf{x}, \mathbf{x}_0) = \int_{\Gamma(\mathbf{x}, \mathbf{x}_0)} \sqrt{\varepsilon_r(\boldsymbol{\xi}(\sigma))}\,d\sigma,$$

where $d\sigma$ is the element of the Euclidian length. For $\mathbf{x} \neq \mathbf{x}_0$ the function $\tau(\mathbf{x}, \mathbf{x}_0)$ is twice continuously differentiable with respect to $\mathbf{x}, \mathbf{x}_0$ and is the solution of the eikonal equation [44, Chapter 3]

$$(2.11) \qquad |\nabla_{\mathbf{x}} \tau(\mathbf{x}, \mathbf{x}_0)|^2 = \varepsilon_r(\mathbf{x}), \ \tau(\mathbf{x}, \mathbf{x}_0) = O(|\mathbf{x} - \mathbf{x}_0|), \quad \mathbf{x} \to \mathbf{x}_0.$$

We assume everywhere below that the geodesic lines are regular [44, Chapter 3]:

Regularity Assumption. *Any two points $\mathbf{x}, \mathbf{x}_0 \in \mathbb{R}^3$ can be connected by a single geodesic line $\Gamma(\mathbf{x}, \mathbf{x}_0)$.*

A sufficient condition guaranteeing the regularity of geodesic lines can be found in [45]. Let $\mu_a(\mathbf{x})$ and $\mu_s(\mathbf{x})$ be the absorption and scattering coefficients of light respectively and let

$$(2.12) \qquad \begin{array}{c} \mu_a(\mathbf{x}), \mu_s(\mathbf{x}) \geq 0, \quad \mu_a(\mathbf{x}), \mu_s(\mathbf{x}) \in C^1(\mathbb{R}^3), \\ \mu_a(\mathbf{x}) = \mu_s(\mathbf{x}) = 0, \quad \mathbf{x} \in \mathbb{R}^3 \setminus \Omega, \\ a(\mathbf{x}) = \mu_a(\mathbf{x}) + \mu_s(\mathbf{x}). \end{array}$$

The function $a(\mathbf{x})$ is the attenuation coefficient. By (2.12)

$$(2.13) \qquad a(\mathbf{x}) \geq 0, \ \mathbf{x} \in \mathbb{R}^3, \ a(\mathbf{x}) \in C^1(\mathbb{R}^3), \quad a(\mathbf{x}) = 0, \ \mathbf{x} \in \mathbb{R}^3 \setminus \Omega.$$

Let $\widetilde{A} = \max(A, d)$. Introduce three domains G, G_a^+ and G_a^-,

(2.14) $$G = \left\{ \mathbf{x} : -\widetilde{A} < x, y < \widetilde{A}, z \in (0, b) \right\}, G_a^+ = G \cup \{z > a\}, G_a^- = G \setminus G_a^+.$$

Below we write sometimes $u(\mathbf{x}, \alpha)$ instead of $u(\mathbf{x}, \mathbf{x}_\alpha)$.

The Forward Problem. *Find the solution $u(\mathbf{x}, \alpha) \in C^1\left(G \times [-d, d] \right)$ of the following problem:*

(2.15) $$\left(\nabla_{\mathbf{x}} \tau(\mathbf{x}, \mathbf{x}_\alpha) / \sqrt{\varepsilon_r(\mathbf{x})} \right) \cdot \nabla_{\mathbf{x}} u(\mathbf{x}, \alpha) + a(\mathbf{x}) u(\mathbf{x}, \alpha) =$$
$$= \mu_s(\mathbf{x}) \int_{\Gamma_d} K(\mathbf{x}, \alpha, \beta) u(\mathbf{x}, \beta) d\beta + f(\mathbf{x} - \mathbf{x}_\alpha), \quad \mathbf{x} \in G, \mathbf{x}_\alpha \in \Gamma_d,$$

(2.16) $$u(\mathbf{x}_\alpha, \mathbf{x}_\alpha) = 0 \text{ for } \mathbf{x}_\alpha \in \Gamma_d.$$

Definition 2.1. *We call equation (2.15) the Riemannian Radiative Transfer Equation (RRTE).*

In (2.15), (2.16) $u(\mathbf{x}, \alpha)$ denotes the steady-state radiance at the point $\mathbf{x}$ generated by the source function $f(\mathbf{x} - \mathbf{x}_\alpha)$. The kernel $K(\mathbf{x}, \alpha, \beta)$ of the integral operator in (2.15) is called the "phase function" [22],

(2.17) $$K(\mathbf{x}, \alpha, \beta) \geq 0, \quad \mathbf{x} \in \overline{\Omega}; \quad \alpha, \beta \in [-d, d],$$
$$K(\mathbf{x}, \alpha, \beta) \in C^1\left(\overline{\Omega} \times [-d, d]^2 \right).$$

Coefficient Inverse Problem. *Let the function $u(\mathbf{x}, \alpha) \in C^1(\overline{\Omega} \times [-d, d])$ be the solution of the Forward Problem. Assume that the coefficient $a(\mathbf{x})$ of equation (2.15) is unknown. Determine the function $a(\mathbf{x})$, assuming that the following function $g(\mathbf{x}, \alpha)$ is known:*

(2.18) $$g(\mathbf{x}, \alpha) = u(\mathbf{x}, \alpha), \quad \forall \mathbf{x} \in \partial\Omega \setminus \partial_1\Omega, \quad \forall \alpha \in (-d, d).$$

3. Existence and Uniqueness Theorem for the Forward Problem. Consider the unit tangent vector ν to the geodesic line $\Gamma(\mathbf{x}, \mathbf{x}_\alpha)$ at the point $\mathbf{x}$ [44, Chapter 3]

$$\nu = \nabla_{\mathbf{x}} \tau(\mathbf{x}, \mathbf{x}_\alpha) / \sqrt{\varepsilon_r(\mathbf{x})}.$$

Hence, the directional derivative $D_\nu q$ of an appropriate function $q(\mathbf{x}, \alpha)$ in the direction of the vector ν is

(3.1) $$D_\nu q = \frac{\nabla_{\mathbf{x}} \tau(\mathbf{x}, \mathbf{x}_\alpha)}{\sqrt{\varepsilon_r(\mathbf{x})}} \cdot \nabla_{\mathbf{x}} q(\mathbf{x}, \alpha).$$

Hence, if the function $q(\mathbf{x}, \mathbf{x}_\alpha)$ solves problem (3.2), then q is given by formula (3.3), where

(3.2) $$\frac{\nabla_{\mathbf{x}} \tau(\mathbf{x}, \mathbf{x}_\alpha)}{\sqrt{\varepsilon_r(\mathbf{x})}} \cdot \nabla_{\mathbf{x}} q(\mathbf{x}, \mathbf{x}_\alpha) = a(\mathbf{x}), \quad q(\mathbf{x}_\alpha, \mathbf{x}_\alpha) = 0,$$

$$(3.3) \qquad q(\mathbf{x}, \mathbf{x}_\alpha) = \int\limits_{\Gamma(\mathbf{x}, \mathbf{x}_\alpha)} a\left(\boldsymbol{\xi}(\sigma)\right) d\sigma.$$

Let

$$(3.4) \qquad p(\mathbf{x}, \mathbf{x}_\alpha) = \exp\left(\int\limits_{\Gamma(\mathbf{x}, \mathbf{x}_\alpha)} a\left(\boldsymbol{\xi}(\sigma)\right) d\sigma\right).$$

Then (3.1)-(3.4) imply:

$$(3.5) \qquad D_\nu p = a\left(\mathbf{x}\right) p.$$

Multiply both sides of equation (2.15) by p and use (3.1)-(3.5). Note that by (2.5) and (2.12) $p(\mathbf{x}, \mathbf{x}_\alpha) f(\mathbf{x} - \mathbf{x}_\alpha) = f(\mathbf{x} - \mathbf{x}_\alpha)$. We obtain

$$
\begin{aligned}
& pD_\nu u + a\left(\mathbf{x}\right) pu = \mu_s(\mathbf{x}) p \int\limits_{\Gamma_d} K(\mathbf{x}, \alpha, \beta) u(\mathbf{x}, \beta) d\beta + f(\mathbf{x} - \mathbf{x}_\alpha), \\
(3.6) \qquad & pD_\nu u + a\left(\mathbf{x}\right) pu = D_\nu\left(pu\right) - a\left(\mathbf{x}\right) pu + a\left(\mathbf{x}\right) pu = D_\nu\left(pu\right), \\
& D_\nu\left(pu\right) = \mu_s(\mathbf{x}) p \int\limits_{\Gamma_d} K(\mathbf{x}, \alpha, \beta) u(\mathbf{x}, \beta) d\beta + f(\mathbf{x} - \mathbf{x}_\alpha).
\end{aligned}
$$

Let the equation of the geodesic line $\Gamma(\mathbf{x}, \mathbf{x}_\alpha)$ be $\boldsymbol{\xi} = \boldsymbol{\xi}(\sigma, \alpha) \in \Gamma(\mathbf{x}, \mathbf{x}_\alpha)$, where σ is the Euclidean length of the part $\Gamma_{\boldsymbol{\xi}}(\mathbf{x}, \mathbf{x}_\alpha)$ of the curve $\Gamma(\mathbf{x}, \mathbf{x}_\alpha)$, which connects points $\boldsymbol{\xi}$ and $\mathbf{x}_\alpha$. Integrating the last line of (3.6) along the vector ν and taking into account the initial condition (2.16), we obtain for $\mathbf{x} \in G, \mathbf{x}_\alpha \in \Gamma_d$

$$
\begin{aligned}
u(\mathbf{x}, \mathbf{x}_\alpha) = & u_0(\mathbf{x}, \mathbf{x}_\alpha) + p^{-1}(\mathbf{x}, \mathbf{x}_\alpha) \times \\
(3.7) \qquad \times & \int\limits_{\Gamma(\mathbf{x}, \mathbf{x}_\alpha)} p(\boldsymbol{\xi}(\sigma, \alpha), \mathbf{x}_\alpha) \mu_s(\boldsymbol{\xi}(\sigma, \alpha)) \left(\int\limits_{\Gamma_d} K(\boldsymbol{\xi}(\sigma, \alpha), \alpha, \beta) u(\boldsymbol{\xi}(\sigma, \alpha), \beta) d\beta\right) d\sigma, \\
& u_0(\mathbf{x}, \mathbf{x}_\alpha) = p^{-1}(\mathbf{x}, \mathbf{x}_\alpha) \int\limits_{\Gamma(\mathbf{x}, \mathbf{x}_\alpha)} f(\boldsymbol{\xi}(\sigma, \alpha) - \mathbf{x}_\alpha) d\sigma.
\end{aligned}
$$

Thus, we conclude that the solution of the Forward Problem (2.15), (2.16) is equivalent to the solution of integral equation (3.7).

Theorem 1. *Assume that conditions (2.12) and (2.17) hold. Then there exists unique solution* $u(\mathbf{x}, \alpha) \in C^1\left(G \times [d, d]\right)$ *of problem (2.15), (2.16). Furthermore, the following inequality is valid:*

$$(3.8) \qquad u(\mathbf{x}, \alpha) \geq m > 0 \text{ for } (\mathbf{x}, \alpha) \in \left(\overline{G}_a^+ \times [-d, d]\right),$$

$$(3.9) \qquad m = \min_{(\mathbf{x}, \alpha) \in \left(\overline{G}_a^+ \times [-d, d]\right)} u_0(\mathbf{x}, \alpha),$$

where the domain G_a^+ is defined in (2.14). Solution of problem (2.15), (2.16) is equivalent to the solution of equation (3.7).

Proof. The equivalency was proven above in this section. Let $\mathbf{x}^*$ be the intersection point of the geodesic line $\Gamma(\mathbf{x}, \mathbf{x}_\alpha)$ with plane $\{z = a\}$. Note that by (2.1), (2.2) and (2.8) $\Gamma(\mathbf{x}^*, \mathbf{x}_\alpha)$ is an interval of a straight line. Since by (2.1), (2.12) and (2.14) $\mu_s(\mathbf{x}) = 0$ for $\mathbf{x} \in G_a^-$, then the first two lines of (3.7) can be rewritten as:

$$u(\mathbf{x}, \mathbf{x}_\alpha) = u_0(\mathbf{x}, \mathbf{x}_\alpha)+$$

(3.10)
$$+p^{-1}(\mathbf{x}, \mathbf{x}_\alpha) \int\limits_{\Gamma(\mathbf{x}, \mathbf{x}^\star)} \left(\int\limits_{\Gamma_d} \widehat{K}(\boldsymbol{\xi}(\sigma, \alpha), \alpha, \beta) u(\boldsymbol{\xi}(\sigma, \alpha), \beta) d\beta \right) d\sigma,$$

where the function $u_0(\mathbf{x}, \mathbf{x}_\alpha)$ is given in the third line of (3.7) and

(3.11)
$$\widehat{K}(\mathbf{x}, \alpha, \beta) = p(\mathbf{x}, \mathbf{x}_\alpha) \mu_s(\mathbf{x}) K(\mathbf{x}, \alpha, \beta).$$

Consider now equations of the geodesic lines. Denote

(3.12)
$$q_1 = \tau_x(\mathbf{x}, \mathbf{x}_\alpha), \ \ q_2 = \tau_y(\mathbf{x}, \mathbf{x}_\alpha), \ \ q_3 = \tau_z(\mathbf{x}, \mathbf{x}_\alpha).$$

Then formulas (3.4) and (3.7) of [44, Chapter 3] imply that equations of geodesic lines are:

(3.13)
$$\frac{dx}{ds} = \frac{q_1}{\varepsilon_r}, \frac{dy}{ds} = \frac{q_2}{\varepsilon_r}, \frac{dz}{ds} = \frac{q_3}{\varepsilon_r},$$

$$\frac{dq_1}{ds} = \frac{\partial_x \varepsilon_r}{2\varepsilon_r}, \frac{dq_2}{ds} = \frac{\partial_y \varepsilon_r}{2\varepsilon_r}, \frac{dq_3}{ds} = \frac{\partial_z \varepsilon_r}{2\varepsilon_r},$$

where $ds = \sqrt{\varepsilon_r(\mathbf{x}(\sigma))} d\sigma$ is the element of the Riemannian length. In the integral (3.10),

(3.14)
$$\mathbf{x}(\sigma, \alpha) = (x(\sigma, \alpha), y(\sigma, \alpha), z(\sigma, \alpha)) \in \Omega.$$

It follows from (2.9) and [37, Lemma 5.1] that there exists a number $c > 0$ such that

(3.15)
$$\tau_z(\mathbf{x}, \mathbf{x}_\alpha) \geq c.$$

Hence, a combination of equation (3.12) with the last equation in (3.13) implies:

(3.16)
$$\partial_s z(s, \alpha) > 0 \text{ and } \partial_\sigma z(\sigma, \alpha) > 0.$$

Consider the equation of the geodesic line $\Gamma(\mathbf{x}, \mathbf{x}^\star)$ in the form:

(3.17)
$$\boldsymbol{\xi}(\sigma, \alpha) = (\xi(\sigma, \alpha), \eta(\sigma, \alpha), \zeta(\sigma, \alpha))$$

Change variables in (3.17) by replacing the variable σ with the variable $\zeta = \zeta(\sigma, \alpha)$. Let $\sigma = \sigma(\zeta, \alpha)$ be the inverse function. Then the equation of the geodesic line $\Gamma(\mathbf{x}, \mathbf{x}^\star)$ can be rewritten as

$$\boldsymbol{\xi} = \widehat{\boldsymbol{\xi}}(\zeta, \alpha) = \boldsymbol{\xi}(\sigma(\zeta, \alpha), \alpha) = (\xi(\sigma(\zeta, \alpha), \alpha), \eta(\sigma(\zeta, \alpha), \alpha), \zeta), \quad \zeta \in (a, z).$$

By (3.14), (3.16) and (3.17) the inverse function $\sigma = \sigma(\zeta, \alpha)$ is monotonically increasing with respect to ζ along the geodesic line $\Gamma(x, x^\star)$, i.e. $\partial_\zeta \sigma(\zeta, \alpha) > 0$. Hence, we change variables in the integral of (3.10) as: $\sigma \Leftrightarrow \zeta = \zeta(\sigma, \alpha)$. Then equation (3.10) can be rewritten as:

$$(3.18) \qquad u(\mathbf{x}, \mathbf{x}_\alpha) = u_0(\mathbf{x}, \mathbf{x}_\alpha) + \int_a^z \left(\int_{\Gamma_d} \widetilde{K}(\mathbf{x}, \widehat{\boldsymbol{\xi}}(\zeta, \alpha), \alpha, \beta, \zeta) u(\widehat{\boldsymbol{\xi}}(\zeta, \alpha), \beta) d\beta \right) d\zeta,$$

where $\mathbf{x} \in G_a^+, \mathbf{x}_\alpha \in \Gamma_d$ and by (3.11)

$$(3.19) \qquad \widetilde{K}(\mathbf{x}, \boldsymbol{\xi}, \alpha, \beta, \zeta) = \frac{1}{p(\mathbf{x}, \mathbf{x}_\alpha)} \widehat{K}(\boldsymbol{\xi}, \alpha, \beta) \partial_\zeta \sigma(\zeta, \alpha).$$

Since we have the integral

$$\int_a^z (...) d\zeta$$

in equation (3.18), then this is the integral equation of the Volterra type. It follows from (2.7), (2.17), (3.4), (3.11)-(3.13) and (3.19) that the kernel of equation (3.18) is a non negative continuously differentiable function of its variables $(\mathbf{x}, \alpha, \beta, z) \in \overline{G}_a^+ \times \overline{\Gamma}_d \times \overline{\Gamma}_d \times [a, b]$. Hence, there exists a number $K_0 > 0$ such that in (3.18), (3.19)

$$(3.20) \qquad 0 \le \widetilde{K}(\mathbf{x}, \boldsymbol{\xi}, \alpha, \beta, \zeta) \le K_0 < \infty \text{ in (3.18).}$$

Since equation (3.18) is of the Volterra type, then its solution can be obtained iteratively as:

$$(3.21) \qquad u_n(\mathbf{x}, \mathbf{x}_\alpha) = \int_a^z \int_{\Gamma_d} \widetilde{K}(\mathbf{x}, \widehat{\boldsymbol{\xi}}(\zeta, \alpha), \alpha, \beta, \zeta) u_{n-1}(\widehat{\boldsymbol{\xi}}(\zeta, \alpha), \beta) d\beta d\zeta,$$
$$u(\mathbf{x}, \mathbf{x}_\alpha) = \sum_{n=0}^\infty u_n(\mathbf{x}, \mathbf{x}_\alpha).$$

It follows from (2.3), (2.4), (3.9) and (3.18)-(3.21) that

$$(3.22) \qquad m \le u(\mathbf{x}, \mathbf{x}_\alpha) \le \left[\max_{(\mathbf{x}, \alpha) \in (G_a^+ \times [-d, d])} u_0(\mathbf{x}, \mathbf{x}_\alpha) \right] \times$$
$$\times \sum_{n=0}^\infty (2dK_0(z - a))^n / n!, \ \mathbf{x} \in G_a^+,$$

where numbers m and K_0 are defined in (3.9) and (3.20) respectively. Estimate (3.8) follows from (3.22). Obviously the series of first derivatives of terms of (3.21) with respect to any of variables x, y, z, α also converges absolutely. Hence the function $u(\mathbf{x}, \mathbf{x}_\alpha)$ in (3.21) belongs to $C^1\left(\overline{G}_a^+ \times \overline{\Gamma}_d\right)$. We set

$$u(\mathbf{x}, \mathbf{x}_\alpha) = \begin{cases} \text{the right hand side of (3.21) for } (\mathbf{x}, \mathbf{x}_\alpha) \in G_a^+ \times \Gamma_d, \\ u_0(\mathbf{x}, \mathbf{x}_\alpha) \text{ for } (\mathbf{x}, \mathbf{x}_\alpha) \in G_a^- \times \Gamma_d. \end{cases}$$

Hence, the so defined function $u(\mathbf{x}, \mathbf{x}_\alpha) \in C^1\left(\overline{G} \times \overline{\Gamma}_d\right)$. Thus, we have proven the existence of the solution $u(\mathbf{x}, \alpha) \in C^1\left(\overline{G} \times [d, d]\right)$ of the Forward Problem (2.15), (2.16) as well as estimate (3.8). To prove uniqueness, one should set in (3.18) $u_0\left(\mathbf{x}, \mathbf{x}_\alpha\right) \equiv 0$ and then proceed in the classical way of the proof of the uniqueness of the Volterra integral equation of the second kind. $\square$

Remark 3.1. *It follows from (3.7) and Theorem 1 that one can solve Forward Problem via the solution of the linear integral equation in (3.7). This is how we solve the forward problem (2.15), (2.16) in the numerical section 6 to generate the data for the inverse problem.*

4. Convexification Numerical Method for the Coefficient Inverse Problem.

4.1. An integral differential equation without the unknown coefficient $a(\mathbf{x})$. By (2.3)-(2.5) equation (2.15) can be rewritten as:

(4.1)
$$
\begin{aligned}
&\left(\nabla_\mathbf{x}\tau(\mathbf{x}, \mathbf{x}_\alpha)/\sqrt{\varepsilon_r(\mathbf{x})}\right) \cdot \nabla_\mathbf{x}u(\mathbf{x}, \alpha) + a(\mathbf{x})u(\mathbf{x}, \alpha) = \\
&= \mu_s(\mathbf{x}) \int\limits_{\Gamma_d} K(\mathbf{x}, \alpha, \beta)u(\mathbf{x}, \beta)d\beta, \quad (\mathbf{x}, \alpha) \in \Omega \times (-d, d).
\end{aligned}
$$

It follows from (3.8) that we can consider a new function $v(\mathbf{x}, \alpha)$,

(4.2)
$$
v(\mathbf{x}, \alpha) = \ln u(\mathbf{x}, \alpha), \quad (\mathbf{x}, \alpha) \in \Omega \times (-d, d).
$$

By (4.2) $u(\mathbf{x}, \alpha) = e^{v(\mathbf{x}, \alpha)}$. Substituting this in (4.1), we obtain for $(\mathbf{x}, \alpha) \in \Omega \times (-d, d)$:

(4.3)
$$
\left(\nabla_\mathbf{x}\tau(\mathbf{x}, \mathbf{x}_\alpha)/\sqrt{\varepsilon_r(\mathbf{x})}\right) \cdot \nabla_\mathbf{x}v(\mathbf{x}, \alpha) + a(\mathbf{x}) = e^{-v(\mathbf{x}, \alpha)}\mu_s(\mathbf{x}) \int\limits_{\Gamma_d} K(\mathbf{x}, \alpha, \beta)e^{v(\mathbf{x}, \beta)}d\beta.
$$

In particular, (4.3) implies that we can calculate the function $a(\mathbf{x})$ by the following formula:

(4.4)
$$
\begin{aligned}
a(\mathbf{x}) = &-\int\limits_{\Gamma_d} \left(\nabla_\mathbf{x}\tau(\mathbf{x}, \mathbf{x}_\alpha)/\sqrt{\varepsilon_r(\mathbf{x})}\right) \cdot \nabla_\mathbf{x}v(\mathbf{x}, \alpha)d\alpha + \\
&+ \int\limits_{\Gamma_d} \left(e^{-v(\mathbf{x}, \alpha)}\mu_s(\mathbf{x}) \int\limits_{\Gamma_d} K(\mathbf{x}, \alpha, \beta)e^{v(\mathbf{x}, \beta)}d\beta\right)d\alpha.
\end{aligned}
$$

Hence, we now focus on the problem of the reconstruction of the function $v(\mathbf{x}, \alpha)$ from the function $g(\mathbf{x}, \alpha)$ given in (2.18). We have

(4.5)
$$
\frac{\tau_z(\mathbf{x}, \alpha)}{\sqrt{\varepsilon_r(\mathbf{x})}}v_z(\mathbf{x}, \alpha) = \frac{\partial}{\partial z}\left(\frac{\tau_z}{\sqrt{\varepsilon_r}}v\right) - \frac{\partial}{\partial z}\left(\frac{\tau_z}{\sqrt{\varepsilon_r}}\right)v.
$$

Introduce a new function $w(\mathbf{x}, \alpha)$ and express $v(\mathbf{x}, \alpha)$ through $v(\mathbf{x}, \alpha)$,

(4.6)
$$
\begin{aligned}
w(\mathbf{x}, \alpha) &= \left(\tau_z(\mathbf{x}, \alpha)/\sqrt{\varepsilon_r(\mathbf{x})}\right)v(\mathbf{x}, \alpha), \\
v(\mathbf{x}, \alpha) &= \left(\sqrt{\varepsilon_r(\mathbf{x})}/\tau_z(\mathbf{x}, \alpha)\right).
\end{aligned}
$$

It follows from (3.15) that the second line of formula (4.6) makes sense. Thus, (4.5) becomes

$$(4.7) \qquad \frac{\tau_z}{\sqrt{\varepsilon_r}} v_z = w_z - \left[\frac{\partial}{\partial z} \left(\frac{\tau_z}{\sqrt{\varepsilon_r}} \right) \frac{\sqrt{\varepsilon_r}}{\tau_z} \right] w.$$

Using (4.6), transform other terms of the differential operator in (4.3),

$$(4.8) \qquad \frac{\tau_x}{\sqrt{\varepsilon_r}} v_x = \frac{\tau_x}{\sqrt{\varepsilon_r}} \frac{\partial}{\partial x} \left(\frac{\sqrt{\varepsilon_r}}{\tau_z} w \right) = \frac{\tau_x}{\tau_z} w_x + \left[\frac{\tau_x}{\sqrt{\varepsilon_r}} \frac{\partial}{\partial x} \left(\frac{\sqrt{\varepsilon_r}}{\tau_z} \right) \right] w.$$

And similarly for $\left(\tau_y / \sqrt{\varepsilon_r} \right) v_y$. Hence, (4.3) becomes

$$
\begin{aligned}
(4.9) \qquad & w_z + \left(\tau_x w_x + \tau_y w_y \right) / \tau_z + \\
& + \left[\left(\tau_x / \sqrt{\varepsilon_r} \right) \partial_x \left(\sqrt{\varepsilon_r} / \tau_z \right) + \left(\tau_y / \sqrt{\varepsilon_r} \right) \partial_y \left(\sqrt{\varepsilon_r} / \tau_z \right) - \left(\sqrt{\varepsilon_r} / \tau_z \right) \partial_z \left(\tau_z / \sqrt{\varepsilon_r} \right) \right] w - \\
& - \exp \left(-w \sqrt{\varepsilon_r} / \tau_z \right) (\mathbf{x}, \alpha) \mu_s(\mathbf{x}) \int_{\Gamma_d} K(\mathbf{x}, \alpha, \beta) \exp \left(w \sqrt{\varepsilon_r} / \tau_z \right) (\mathbf{x}, \beta) d\beta = \\
& = -a(\mathbf{x}), \quad (\mathbf{x}, \alpha) \in \Omega \times (-d, d).
\end{aligned}
$$

Differentiate both sides of (4.9) with respect to α and use $\partial_\alpha a(\mathbf{x}) \equiv 0$. We obtain for $(\mathbf{x}, \alpha) \in \Omega \times (-d, d)$:

$$
\begin{aligned}
(4.10) \qquad & \partial_\alpha w_z + \partial_\alpha \left(\left(\tau_x w_x + \tau_y w_y \right) / \tau_z \right) + \\
& + \partial_\alpha \left\{ \left[\left(\tau_x / \sqrt{\varepsilon_r} \right) \partial_x \left(\sqrt{\varepsilon_r} / \tau_z \right) + \left(\tau_y / \sqrt{\varepsilon_r} \right) \partial_y \left(\sqrt{\varepsilon_r} / \tau_z \right) \right] w \right\} - \\
& - \partial_\alpha \left[\left(\sqrt{\varepsilon_r} / \tau_z \right) \partial_z \left(\tau_z / \sqrt{\varepsilon_r} \right) w \right] - \\
& - \partial_\alpha \left[\exp \left(-w \sqrt{\varepsilon_r} / \tau_z \right) (\mathbf{x}, \alpha) \mu_s(\mathbf{x}) \int_{\Gamma_d} K(\mathbf{x}, \alpha, \beta) \exp \left(w \sqrt{\varepsilon_r} / \tau_z \right) (\mathbf{x}, \beta) d\beta \right] = 0.
\end{aligned}
$$

The Dirichlet boundary condition for the function $w(\mathbf{x}, \alpha)$ is:

$$(4.11) \qquad w(\mathbf{x}, \alpha) = \frac{\tau_z(\mathbf{x}, \alpha)}{\sqrt{\varepsilon_r(\mathbf{x})}} \ln g_1(\mathbf{x}, \alpha), \quad (\mathbf{x}, \alpha) \in \partial\Omega \times (-d, d),$$

$$(4.12) \qquad g_1(\mathbf{x}, \alpha) = \begin{cases} g(\mathbf{x}, \alpha), & \mathbf{x} \in \partial\Omega \backslash \partial_1\Omega, \quad \alpha \in (-d, d), \\ u_0(\mathbf{x}, \alpha), & \mathbf{x} \in \partial_1\Omega, \quad \alpha \in (-d, d). \end{cases}$$

Thus, we develop below a numerical method to obtain an approximate solution $w(\mathbf{x}, \alpha)$ of problem (4.10)-(4.12).

4.2. A special orthonormal basis in $L_2(-d, d)$. First, we introduce a special orthonormal basis in $L_2(-d, d)$, which was first discovered in [31], also, see [33, section 6.2.3]. Consider a linearly independent set of functions $\{\alpha^n e^\alpha\}_{n=0}^\infty \subset L_2(-d, d)$, which is complete in $L_2(-d, d)$. The Gram-Schmidt orthonormalization procedure being applied to this set, results in the orthonormal basis $\{\Psi_n(\alpha)\}_{n=0}^\infty$ in $L_2(-d, d)$. The Gram-Schmidt procedure is unstable when it is applied to an infinite number of functions. However, we have not seen an instability when applying it to a relatively small number of functions for $n \in [0, 12]$. The same was observed in a number of previous publications of this research group, see, e.g. [26, 34], [33, Chapters 7,10,12].

Let $[,]$ be the scalar product in $L_2(-d, d)$. Denote $b_{s,k} = [Q'_s, Q_k]$. Then [31], [33, section 6.2.3]

$$(4.13) \qquad b_{s,k} = \begin{cases} 1, s = k, \\ 0, s > k. \end{cases}$$

Consider the $N \times N$ matrix $B_N = (b_{s,k})_{(s,k)=(0,0)}^{(N-1,N-1)}$. Then (4.13) implies that $\det B_N = 1$, which means that this matrix is invertible. In fact, the existence of the matrix B_N^{-1} for each $N \geq 1$ is the key property why the basis $\{Q_n(\alpha)\}_{n=0}^{\infty}$ was originally constructed in [31]. Indeed, consider, for example either the basis of standard orthonormal polynomials or the basis of trigonometric functions. In each of these, the first function is an identical constant, which means that the first raw of an analog of the matrix B_N is zero.

4.3. A boundary value problem for a system of nonlinear PDEs. We assume that the functions $w(\mathbf{x}, \alpha)$, $w_\alpha(\mathbf{x}, \alpha)$ can be represented as truncated Fourier-like series

$$(4.14) \qquad w(\mathbf{x}, \alpha) = \sum_{n=0}^{N-1} w_n(\mathbf{x}) Q_n(\alpha), \quad w_\alpha(\mathbf{x}, \alpha) = \sum_{n=0}^{N-1} w_n(\mathbf{x}) Q'_n(\alpha)$$

with unknown coefficients $\{w_n(\mathbf{x})\}_{n=0}^{N-1}$. Thus, we focus below on the computation of the $N-D$ vector function

$$(4.15) \qquad V(\mathbf{x}) = (w_0, w_1, \cdots, w_{N-1})^T (\mathbf{x}).$$

Remarks 4.1:
1. *The representations (4.14) mean that this is a version of the Galerkin method. However, unlike classical well-posed forward problems for PDEs, where Galerkin method is used and its convergence at $N \to \infty$ is usually proven, we cannot prove convergence of our inversion numerical procedure described below for $N \to \infty$. This is basically because of the ill-posed nature of our CIP. Thus, we actually work below within the framework of an approximate mathematical model. Then, however, the question can be raised whether this model really works numerically. The answer is positive, and this answer is obtained computationally in section 6. We observe that very similar truncated series were used in some other above cited works on the convexification, such as, e.g. [26, 34], [33, Chapters 7,10], and all of them have demonstrated good numerical performances. Likewise, truncated Fourier series were used in works of other authors about CIPs, such as, e.g. [20, 24, 25, 42] and also without proofs of convergence of inversion procedures at $N \to \infty$. Those proofs were not provided for the same reason as the one here: the ill-posed nature of CIPs.*
2. *Finally, we refer to subsection 3.4 of [34] for more arguments in support of those of item 1. In particular, these arguments include the well known fact that the Huygens-Fresnel theory of the diffraction in optics is not yet rigorously derived from the Maxwell's equations, see, e.g. a classic textbook [9, pages 412, 413]. Philosophically, this fact is similar with the discussion of item 1.*

Substitute (4.14) in (4.10). Next, sequentially multiply the obtained equation by $Q_n(\alpha)$, $n = 0, ..., N - 1$ and integrate with respect to $\alpha \in (-d, d)$. We obtain the following system of coupled quasilinear integral differential equations

$$(4.16) \qquad B_N V_z(\mathbf{x}) + A_1(\mathbf{x})V_x(\mathbf{x}) + A_2(\mathbf{x})V_y(\mathbf{x}) + F(V(\mathbf{x}), \mathbf{x}) = 0, \qquad \mathbf{x} \in \Omega,$$

where $A_1(\mathbf{x})$ and $A_2(\mathbf{x})$ are $N \times N$ matrices and $F(V(\mathbf{x}), \mathbf{x})$ is a certain vector function, which depends nonlinearly on $V(\mathbf{x})$. Explicit formulas for $A_1(\mathbf{x})$, $A_2(\mathbf{x})$ and $F(V(\mathbf{x}), \mathbf{x})$ can be easily written. However, we do not present them here for brevity. In addition, the boundary condition for the vector function $V(\mathbf{x})$ is:

$$(4.17) \qquad V(\mathbf{x})\,|_{\partial\Omega} = P(\mathbf{x}) = (p_0, p_1, \cdots, p_{N-1})^T(\mathbf{x}),$$

$$(4.18) \qquad p_n(\mathbf{x}) = \int_{-d}^{d} \left[\frac{\tau_z(\mathbf{x}, \alpha)}{\sqrt{\varepsilon_r(\mathbf{x})}} \ln[g_1(\mathbf{x}, \alpha)] \right] Q_n(\alpha)d\alpha, \quad n = 0, 1, \cdots, N - 1.$$

Thus, we now have to solve the boundary value problem (4.16)-(4.18).

To numerically calculate the derivatives of $\nabla_{\mathbf{x}}\tau(\mathbf{x}, \alpha)$ with respect to α, we represent $\nabla_{\mathbf{x}}\tau(\mathbf{x}, \alpha)$ via the truncated Fourier series with respect to the above basis $\{Q_n(\alpha)\}_{n=0}^{N-1}$ as:

$$(4.19) \qquad \nabla_{\mathbf{x}}\tau(\mathbf{x}, \alpha) = \sum_{n=0}^{N-1} (\nabla_{\mathbf{x}}\tau)_n(\mathbf{x})Q_n(\alpha).$$

Then we use explicit formulas for functions $Q_n(\alpha)$ to get

$$(4.20) \qquad \partial_\alpha(\nabla_{\mathbf{x}}\tau) = \sum_{n=0}^{N-1} (\nabla_{\mathbf{x}}\tau)_s(\mathbf{x})Q_n'(\alpha).$$

Then equations (4.19) and (4.20) are used in (4.16)-(4.18). Thus, it follows from (4.10) and (4.14)-(4.20) that

$$(4.21) \qquad \begin{cases} A_1(\mathbf{x}), A_2(\mathbf{x}) \in C_{N^2}(\overline{\Omega}), \text{ and the vector function} \\ \quad F(V(\mathbf{x}), \mathbf{x}) \text{ is continuously differentiable} \\ \quad\quad \text{with respect to its arguments for } \mathbf{x} \in \overline{\Omega}. \end{cases}$$

Here and below for any integer $k \geq 2$ and for any Banach space B we denote $B_k = B^k$ with the norm $\|f\|_{B_k}^2 = \|f_1\|_B^2 + ... + \|f_k\|_B^2$, $\forall f = (f_1, ..., f_k)^T \in B_k$.

4.4. Minimization problem. Let $R > 0$ be an arbitrary number and the vector function $P(x)$ be the boundary condition in (4.17). Define the set $S(R, P) \subset H_N^1(\Omega)$ as:

$$(4.22) \qquad S(R, P) = \left\{ V \in H_N^1(\Omega) : V(\mathbf{x})\,|_{\partial\Omega} = P(\mathbf{x}), \|W\|_{H_N^1(\Omega)} < R \right\}.$$

To solve problem (4.16)-(4.18), we solve the following minimization problem:

Minimization Problem 1. *Let $\lambda \geq 1$ be a parameter. Minimize the following weighted cost functional $J_\lambda(V)$ on the set $\overline{S(R, P)}$:*

$$(4.23) \qquad J_\lambda(V) = \left\| (B_N V_z + A_1(\mathbf{x})V_x(\mathbf{x}) + A_2(\mathbf{x})V_y(\mathbf{x}) + F(V(\mathbf{x}), \mathbf{x}))e^{\lambda z} \right\|_{L_N^2(\Omega)}^2.$$

5. Convergence Analysis. We carry out the convergence analysis for a modified Minimization Problem 1. To obtain this modification, we rewrite the differential operator in functional (4.23) via finite differences with respect to the variables x, y while leaving the conventional derivative with respect to z. We call this "partial finite differences".

5.1. Partial finite differences. Let $m > 1$ be an integer. Let $A > 0$ be the number in (2.2). Consider two partitions of the interval $(-A, A)$,

(5.1)
$$-A = x_0 < x_1 < \cdots < x_m = A, \quad x_{j+1} - x_j = h, \quad j = 0, \cdots, m-1,$$
$$-A = y_0 < y_1 < \cdots < y_m = A, \quad y_{j+1} - y_j = h, \quad j = 0, \cdots, m-1.$$

We assume that

(5.2)
$$h \geq h_0 = const. > 0.$$

Define the semidiscrete subset Ω^h of the domain Ω as:

(5.3)
$$\Omega_1^h = \{(x_i, y_j)\}_{i,j=0}^m,$$

(5.4)
$$\Omega^h = \Omega_1^h \times (a, b) = \left\{(x_i, y_j) : (x_i, y_j) \in \Omega_1^h, z \in (a, b)\right\}.$$

Below points $(x_i, y_j, z) \in \Omega^h$ are denoted as $\mathbf{x}^h$. By (2.2), (5.3) and (5.4) the boundary $\partial\Omega^h$ of the domain Ω^h is:

$$\partial\Omega^h = \partial_1\Omega^h \cup \partial_2\Omega^h \cup \partial_3\Omega^h,$$
$$\partial_1\Omega^h = \Omega_1^h \times \{z = a\}, \quad \partial_2\Omega^h = \Omega_1^h \times \{z = b\},$$
$$\partial_3\Omega^h = \{(x_0, y_j, z), (x_m, y_j, z) : z \in (a, b)\}.$$

Let the vector function $Y(\mathbf{x}) \in C_N^1(\overline{\Omega})$. Denote

$$Y^h(\mathbf{x}^h) = Y(x_i, y_j, z), \quad \mathbf{x}^h = (x_i, y_j, z) \in \Omega^h.$$

Thus, $Y^h(\mathbf{x}^h)$ is an $N - D$ vector function of discrete variables $(x_i, y_j) \in \Omega_1^h$ and continuous variable $z \in (a, b)$. Note that by (5.1) the boundary terms at $\partial_3\Omega^h$ of this vector function, which correspond to $Y(\mathbf{x})|_{\partial_3\Omega^h}$, are:

$$\{Y(x_0, y_j, z)\} \cup \{Y(x_m, y_j, z)\} \cup \{Y(x_i, y_0, z)\} \cup \{Y(x_i, y_m, z)\}, i, j = 0, \cdots, m.$$

For two vector functions $Y^{(1)}(\mathbf{x}) = \left(Y_0^{(1)}(\mathbf{x}), \cdots, Y_{N-1}^{(1)}(\mathbf{x})\right)^T$ and $Y^{(2)}(\mathbf{x}) = (Y_0^{(2)}(\mathbf{x}), \cdots, Y_{N-1}^{(2)}(\mathbf{x}))^T$ their scalar product $Y^{(1)}(\mathbf{x}) \cdot Y^{(2)}(\mathbf{x})$ is defined as the scalar product in $\mathbb{R}^N$, and $(Y(\mathbf{x}))^2 = Y(\mathbf{x}) \cdot Y(\mathbf{x})$. Respectively,

$$Y^{(1)h}(\mathbf{x}^h) \cdot Y^{(2)h}(\mathbf{x}^h) =$$

(5.5)
$$= \sum_{n=0}^{N-1} \sum_{(i,j)=(1,1)}^{(i,j)=(m-1,m-1)} Y_n^{(1)h}(x_i, y_j, z) Y_n^{(2)h}(x_i, y_j, z),$$
$$\left(Y^h(\mathbf{x}^h)\right)^2 = Y^h(\mathbf{x}^h) \cdot Y^h(\mathbf{x}^h), \quad \left|Y^h(\mathbf{x}^h)\right| = \sqrt{Y^h(\mathbf{x}^h) \cdot Y^h(\mathbf{x}^h)}.$$

We will use formulas (5.5) everywhere below without further mentioning. We exclude here boundary terms with $i, j = 0$ and $i, j = m$ since we work below with finite difference derivatives as defined in the next paragraph.

We define finite difference derivatives of the semidiscrete $N-$D vector function $Y^h(\mathbf{x}^h)$ with respect to x, y only at interior points of the domain Ω^h with $i, j = 1, ..., m - 1$,

$$
\begin{aligned}
&\partial_x Y^h (x_i, y_j, z) = Y^h (x_i, y_j, z)_x = \left(Y^h (x_{i+1}, y_j, z) - Y^h (x_{i-1}, y_j, z) \right) / (2h), \\
&\partial_x Y^h (x_i, y_j, z) = Y^h (x_i, y_j, z)_x = \left(Y^h (x_{i+1}, y_j, z) - Y^h (x_{i-1}, y_j, z) \right) / (2h), \\
&\partial_y Y^h (x_i, y_j, z) = Y^h (x_i, y_j, z)_y = \left(Y^h (x_i, y_{j+1}, z) - Y^h (x_i, y_{j-1}, z) \right) / (2h),
\end{aligned}
$$
(5.6)
$$
Y_x^h (\mathbf{x}^h) = \left\{ Y^h (x_i, y_j, z)_x \right\}_{i,j=1}^{m-1}, \ Y_y^h (\mathbf{x}^h) = \left\{ Y^h (x_i, y_j, z)_y \right\}_{i,j=1}^{m-1}.
$$

We need semidiscrete analogs of spaces $C_{N^2} \left(\overline{\Omega} \right), H_N^1 (\Omega), L_N^2 (\Omega)$. All three are defined using the same principle. Hence, we provide here only two definitions: for the space $H_N^{1,h} (\Omega^h)$ and its subspace $H_{N,0}^{1,h} (\Omega^h)$. Others are similar. We introduce the space $H_N^{1,h} (\Omega^h)$ as:

$$
H_N^{1,h} \left(\Omega^h \right) =
$$
(5.7)
$$
= \left\{
\begin{array}{c}
Y^h(\mathbf{x}^h) : \left\| Y^h(\mathbf{x}^h) \right\|_{H_N^{1,h}(\Omega^h)}^2 = \sum\limits_{i,j=1}^{m-1} \int\limits_a^b \left(Y^h (x_i, y_j, z) \right)^2 dz + \\
+ \sum\limits_{i,j=1}^{m-1} \int\limits_a^b \left(Y_x^h (x_i, y_j, z) \right)^2 dz + \sum\limits_{i,j=1}^{m-1} \int\limits_a^b \left(Y_y^h (x_i, y_j, z) \right)^2 dz + \\
+ \sum\limits_{i,j=1}^{m-1} \int\limits_a^b \left(Y_z^h (x_i, y_j, z) \right)^2 dz < \infty
\end{array}
\right\},
$$

(5.8)
$$
H_{N,0}^{1,h} \left(\Omega^h \right) = \left\{ Y^h(\mathbf{x}^h) \in H_N^{1,h} \left(\Omega^h \right) : Y^h(\mathbf{x}^h) \mid_{\partial \Omega^h} = 0 \right\}.
$$

By embedding theorem $H_N^{1,h} (\Omega^h) \subset C_N^h \left(\overline{\Omega}^h \right)$ and

(5.9)
$$
\left\| Y^h(\mathbf{x}^h) \right\|_{C_N^h(\overline{\Omega}^h)} \leq C \left\| Y^h(\mathbf{x}^h) \right\|_{H_N^{1,h}(\Omega^h)}, \forall Y^h \in H_N^{1,h} \left(\Omega^h \right),
$$

where the number $C = C (h_0, A, \Omega) > 0$ depends only on listed parameters, where h_0 is defined in (5.2). Also, it follows from (5.2), (5.6) that

(5.10)
$$
\left\| Y_x^h(\mathbf{x}^h) \right\|_{L^{2,h}(\Omega^h)}, \left\| Y_y^h(\mathbf{x}^h) \right\|_{L^{2,h}(\Omega^h)} \leq C \left\| Y^h(\mathbf{x}^h) \right\|_{L^{2,h}(\Omega^h)}.
$$

The following formulas are semidiscrete analogs of (4.14):

(5.11)
$$
w^h(\mathbf{x}^h, \alpha) = \sum_{n=0}^{N-1} w_n^h(\mathbf{x}^h) Q_n(\alpha), \ \partial_\alpha w^h(\mathbf{x}^h, \alpha) = \sum_{n=0}^{N-1} w_n^h(\mathbf{x}^h) Q_n'(\alpha).
$$

Also, let $V^h(\mathbf{x}^h) = \left(w_0^h, \cdots, w_{N-1}^h\right)^T(\mathbf{x}^h)$. Using (5.6) and (5.11), we now rewrite problem (4.16)-(4.18), in the form of partial finite differences as:

$$
\text{(5.12)} \qquad \begin{array}{c} B_N V_z^h\left(\mathbf{x}^h\right) + A_1^h\left(\mathbf{x}^h\right) V_x^h\left(\mathbf{x}^h\right) + A_2^h\left(\mathbf{x}^h\right) V_y^h\left(\mathbf{x}^h\right) + \\ + F^h\left(V^h\left(\mathbf{x}^h\right), \mathbf{x}^h\right) = 0, \quad \mathbf{x}^h \in \Omega^h, \end{array}
$$

$$
\text{(5.13)} \qquad V^h\left(\mathbf{x}^h\right)\big|_{\partial\Omega^h} = P^h\left(\mathbf{x}^h\right).
$$

Suppose that we have found the vector function $V^h\left(\mathbf{x}^h\right)$ satisfying equation (5.12) and boundary condition (5.13). Then it follows from (4.4), (4.6) and (4.14) that to find the semidiscrete analog $a^h\left(\mathbf{x}^h\right)$ of the unknown coefficient $a\left(\mathbf{x}\right)$, we should use:

$$
\text{(5.14)} \qquad \begin{array}{c} a^h\left(\mathbf{x}^h\right) = \\[4pt] -\left(1/2d\right) \int\limits_{-d}^{d} \left(\nabla_{\mathbf{x}^h}\tau^h/\sqrt{\varepsilon_r^h}\right) \cdot \nabla_{\mathbf{x}^h}\left(\left(\tau_z^h(/\sqrt{\varepsilon_r^h}\right) w^h\right)(\mathbf{x}^h, \alpha)d\alpha + \\[4pt] +\left(1/2d\right) \int\limits_{-d}^{d} \left(r^h(\mathbf{x}^h, \alpha)\mu_s(\mathbf{x}^h) \int\limits_{-d}^{d} K(\mathbf{x}^h, \alpha, \beta)\left(r^h(\mathbf{x}^h, \beta)\right)^{-1} d\beta\right) d\alpha, \\[4pt] r^h(\mathbf{x}^h, \alpha) = \exp\left(-\left(\sqrt{\varepsilon_r}/\tau_z\right)(\mathbf{x}^h) \sum\limits_{n=0}^{N-1} w_n(\mathbf{x}^h)Q_n(\alpha)\right), \quad \mathbf{x}^h \in \Omega^h. \end{array}
$$

Obviously, the following semidiscrete analog of (4.21) is valid:

$$
\text{(5.15)} \qquad \left\{ \begin{array}{c} A_1^h(\mathbf{x}^h), A_2^h(\mathbf{x}^h) \in C_{N^2}^h\left(\overline{\Omega}^h\right) \text{ and the vector function} \\ F^h\left(V^h\left(\mathbf{x}^h\right), \mathbf{x}^h\right) \text{ is continuously differentiable} \\ \text{with respect to its arguments for } \mathbf{x}^h \in \overline{\Omega}^h. \end{array} \right.
$$

Let $M^h = \max\left(\left\|A_1^h(\mathbf{x}^h)\right\|_{C_{N^2}^h}, \left\|A_2^h(\mathbf{x}^h)\right\|_{C_{N^2}^h}\right)$. Then

$$
\text{(5.16)} \qquad M^h \leq M = \max\left(\left\|A_1(\mathbf{x}^h)\right\|_{C_{N^2}^h}, \left\|A_2(\mathbf{x}^h)\right\|_{C_{N^2}^h}\right).
$$

The following functional $J_\lambda^h\left(V^h\right)$ is the semidiscrete analog of the functional $J_\lambda\left(V\right)$ in (4.23):

$$
\text{(5.17)} \qquad J_\lambda^h\left(V^h\right) = \left\|\left(B_N V_z^h + A_1^h V_x^h + A_2^h V_y^h + F^h\left(V^h\left(\mathbf{x}^h\right), \mathbf{x}^h\right)\right) e^{\lambda z}\right\|_{L_N^{2,h}\left(\Omega^h\right)}^2.
$$

Let $R > 0$ be an arbitrary number. Define the semidiscrete analog $S^h\left(R, P^h\right)$ of the set $S\left(R, P\right)$ in (4.22) as:

$$
\text{(5.18)} \qquad \begin{array}{c} S^h\left(R, P^h\right) = \\ = \left\{V^h \in H_N^{1,h}\left(\Omega^h\right) : V^h\left(\mathbf{x}^h\right)\big|_{\partial\Omega^h} = P^h\left(\mathbf{x}^h\right), \left\|V^h\right\|_{H_N^{1,h}\left(\Omega^h\right)} < R\right\}. \end{array}
$$

To find an approximate solution $V^h\left(\mathbf{x}^h\right)$ of problem (5.12), (5.13), we consider the following problem:

Minimization Problem 2. *Minimize the functional $J_\lambda^h\left(V^h\right)$ in (5.17) on the set $\overline{S^h\left(R, P^h\right)}$ defined in (5.18).*

5.2. Formulations of theorems. Lemma 1. *Consider an $n \times n$ matrix D and assume that the inverse matrix D^{-1} exists. Then there exists a number $\xi = \xi\left(D\right) > 0$ such that $\|Dx\|^2 \geq \xi\|x\|^2, \forall x \in \mathbb{R}^n$, where $\|\cdot\|$ is the euclidean norm.*

We omit the proof of this lemma since it is well known.

Theorem 2. (Carleman estimate). *Let M be the number defined in (5.16). Assume that (5.2) holds. There exists a sufficiently large number $\lambda_0 = \lambda_0(d, M, \Omega^h, B_N, \tau^h, \varepsilon_r^h, h_0) \geq 1$ depending only on listed parameters such that the following Carleman estimate holds:*

$$\left\|\left(B_N V_z^h + A_1^h V_x^h + A_2^h V_y^h\right) e^{\lambda z}\right\|_{L_N^{2,h}(\Omega^h)}^2 \geq$$

$$(5.19) \qquad \geq (1/4) \cdot \left\|\left(B_N V_z^h\right) e^{\lambda z}\right\|_{L_N^{2,h}(\Omega^h)}^2 + \left(\lambda^2/8\right) \cdot \left\|\left(B_N V^h\right) e^{\lambda z}\right\|_{L_N^{2,h}(\Omega^h)}^2,$$

$$\forall V^h \in H_{N,0}^{1,h}\left(\Omega^h\right), \forall \lambda \geq \lambda_0.$$

Theorem 3 (central analytical result). *Assume that (5.2) holds and let $S^h\left(R, P^h\right)$ be the set defined in (5.18). Then:*

1. At every point $V^h \in \overline{S^h\left(R, P^h\right)}$ and for every $\lambda \geq 0$ the functional $J_\lambda^h\left(V^h\right)$ defined in (5.17) has the Fré chet derivative $\left(J_\lambda^h\right)'\left(V^h\right) \in H_{N,0}^{1,h}\left(\Omega^h\right)$. Furthermore, the Fréchet derivative $\left(J_\lambda^h\right)'\left(V^h\right)$ satisfies the Lipschitz condition with the number $\rho > 0$ is independent on V_1^h, V_2^h :

$$(5.20) \qquad \left\|\left(J_\lambda^h\right)'\left(V_2^h\right) - \left(J_\lambda^h\right)'\left(V_1^h\right)\right\|_{H_N^{1,h}(\Omega^h)} \leq \rho\left\|V_2^h - V_1^h\right\|_{H_N^{1,h}(\Omega^h)},$$

$$\forall V_1^h, V_2^h \in \overline{S^h\left(R, P^h\right)}.$$

2. There exists a sufficiently large number λ_1

$$(5.21) \qquad \lambda_1 = \lambda_1\left(R, d, M, \Omega^h, B_N, \tau^h, \varepsilon_r^h, h_0\right) \geq \lambda_0 \geq 1$$

depending only on listed parameters such that functional (5.17) is strictly convex on the set $\overline{S\left(R, P^h\right)}$, i.e. there exists a number $C_1 = C_1\left(R, d, M, \Omega^h, B_N, \tau^h, \varepsilon_r^h, h_0\right) > 0$ depending only on listed parameters such that the following inequality holds:

$$(5.22) \qquad J_\lambda^h\left(V_2^h\right) - J_\lambda^h\left(V_1^h\right) - \left(J_\lambda^h\right)'\left(V_1^h\right)\left(V_2^h - V_1^h\right) \geq C_1 \lambda^2 e^{2\lambda a}\left\|V_2^h - V_1^h\right\|_{H_N^{1,h}(\Omega^h)}^2,$$

$$\forall \lambda \geq \lambda_1, \ \forall V_1^h, V_2^h \in \overline{S^h\left(R, P^h\right)}.$$

3. For each $\lambda \geq \lambda_1$ there exists unique minimizer $V_{\min,\lambda}^h \in \overline{S^h\left(R, P^h\right)}$ of the functional $J_\lambda^h\left(V^h\right)$ on the set $\overline{S^h\left(R, P^h\right)}$ and

$$(5.23) \qquad \left(J_\lambda^h\right)'\left(V_{\min,\lambda}^h\right)\left(V^h - V_{\min,\lambda}^h\right) \geq 0, \ \forall V^h \in \overline{S^h\left(R, P^h\right)}.$$

Remark 5.1. *Below $C_1 > 0$ denotes different numbers depending on the same parameters as ones listed above.*

Let $\delta > 0$ be the level of the noise in the data. Our goal now is to estimate the accuracy of the minimizer $V^h_{\min,\lambda}$ depending on δ. Following the classical concept for ill-posed problems [48], we assume the existence of the exact solution

$$(5.24) \qquad V^{h*} \in S^h\left(R, P^{h*}\right)$$

of problem (5.12)-(5.13) with the exact, i.e. noiseless data P^{h*}. Hence,

$$B_N V^{h*}_z\left(\mathbf{x}^h\right) + A^h_1\left(\mathbf{x}^h\right) V^{h*}_x\left(\mathbf{x}^h\right) + A^h_2\left(\mathbf{x}^h\right) V^{h*}_x\left(\mathbf{x}^h\right) +$$

$$(5.25) \qquad + F^h\left(V^{h*}\left(\mathbf{x}^h\right), \mathbf{x}^h\right) = 0, \mathbf{x}^h \in \Omega^h,$$

$$(5.26) \qquad V^{h*}\left(\mathbf{x}^h\right)|_{\partial\Omega^h} = P^{h*}\left(\mathbf{x}^h\right).$$

Let two vector functions $G^{h*}\left(\mathbf{x}^h\right)$ and $G^h\left(\mathbf{x}^h\right)$ be such that

$$(5.27) \qquad G^{h*}\left(\mathbf{x}^h\right) \in S^h\left(R, P^{h*}\right), G^h\left(\mathbf{x}^h\right) \in S^h\left(R, P^h\right),$$

$$(5.28) \qquad \left\|G^h - G^{h*}\right\|_{H^{1,h}_N(\Omega^h)} < \delta.$$

Theorem 4. *Assume that conditions (5.24)-(5.28) hold. Consider the number λ_2,*

$$(5.29) \qquad \lambda_2 = \lambda_1\left(2R, d, M, \Omega^h, B_N, \tau^h, \varepsilon^h_r, h_0\right) \geq \lambda_1,$$

where $\lambda_1\left(2R, d, \Omega^h, M^h, B_N, \tau^h, \varepsilon^h_r, h_0\right)$ is the number in (5.21). Let $V^h_{\min,\lambda_2}$ be the minimizer of functional (5.17) on the set $\overline{S^h\left(R, P^h\right)}$, which was found in Theorem 3. Let $\alpha \in (0, R)$ be a number. Suppose that (5.24) is replaced with

$$(5.30) \qquad V^{h*} \in S^h\left(R - \alpha, P^{h*}\right), \text{ where } \alpha > C_1\delta.$$

Then the vector function $V^h_{\min,\lambda_2}$ belongs to the open set $S^h\left(R, P^h\right)$ and the following accuracy estimate holds:

$$\left\|V^h_{\min,\lambda_2} - V^{h*}\right\|_{H^{1,h}_N(\Omega^h)} \leq C_1\delta.$$

Consider now the gradient descent method of the minimization of functional (5.17) on the set $\overline{S^h\left(R, P^h\right)}$. Let $V^h_0 \in B\left(R/3, P^h\right)$ be an arbitrary point of this set. We take V^h_0 as the starting point of our iterations. Construct the sequence of the gradient descent method as:

$$(5.31) \qquad V^h_n = V^h_{n-1} - \beta\left(J^h_{\lambda_2}\right)'\left(V^h_{n-1}\right), n = 1, 2, \ldots,$$

where $\beta > 0$ is a small number. Since by Theorem 2 functions $\left(J_{\lambda_2}^h\right)'\left(V_{n-1}^h\right) \in H_{N,0}^{1,h}\left(\Omega^h\right)$, then all vector functions V_n^h have the same boundary conditions P^h, see (5.8) and (5.18).

   Theorem 5. *Let conditions of Theorem 4 hold, except that (5.30) is replaced with*

$$V^{h*} \in S^h\left(\frac{R-\alpha}{3}, P^{h*}\right), \text{ where } \alpha/3 > C_1\delta.$$

Then there exists a sufficiently small number $\beta > 0$ and a number $\gamma = \gamma(\beta) \in (0,1)$ such that in (5.31) all functions $V_n^h \in S^h\left(R, P^h\right)$, and the following convergence estimates hold

(5.32)
$$\left\|V_n^h - V_{\min,\lambda_2}^h\right\|_{H_N^{1,h}(\Omega^h)} \leq \beta^n \left\|V_0^h - V_{\min,\lambda_2}^h\right\|_{H_N^{1,h}(\Omega^h)},$$
$$\left\|V_n^h - V^{h*}\right\|_{H_N^{1,h}(\Omega^h)} \leq C_1\delta + \beta^n \left\|V_0^h - V_{\min,\lambda_2}^h\right\|_{H_N^{1,h}(\Omega^h)},$$
$$\left\|a_n^h - a^{h*}\right\|_{L_N^{2,h}(\Omega^h)} \leq C_1\delta + \beta^n \left\|V_0^h - V_{\min,\lambda_2}^h\right\|_{H_N^{1,h}(\Omega^h)},$$

where $a_n^h\left(\mathbf{x}^h\right)$ and $a_n^{h*}\left(\mathbf{x}^h\right)$ are functions which are obtained from V_n^h and V^{h*} respectively via (5.14).

   Remarks 5.2:

   1. *By Remark 1.1 estimates (5.32) imply that the gradient descent method (5.31) of the minimization of the functional $J_\lambda^h\left(V^h\right)$ converges globally for $\lambda = \lambda_2$. Indeed, its starting point V_0^h is an arbitrary point of the set $S\left(R/3, P^h\right)$, and $R > 0$ is an arbitrary number.*

   2. *We fix $\lambda = \lambda_2$ in Theorem 3 only for the sake of the definiteness. In fact, obvious analogs of these theorems are valid for any $\lambda \geq \lambda_2$.*

   3. *Even though above Theorems 3-5 require sufficiently large values of the parameter λ, we have numerically established in our computations in section 7 that actually $\lambda = 5$ is sufficient. A similar observation has been consistently made in all above cited works about the convexification method. Conceptually, this is similar with the well known fact from almost any asymptotic theory. Indeed, such a theory typically claims that if a certain parameter X is sufficiently large/small, then a certain formula Y is valid with a good accuracy. However, for any specific numerical implementation with its specific range of parameters only numerical studies can establish which exactly value of X is sufficient to obtain a good accuracy of Y.*

   4. *Proofs of Theorems 2, 4 and 5 are similar with the proofs in [34] of Theorems 4.1, 4.4 and 4.5 respectively. Therefore, we prove in this paper only Theorem 3.*

   5.3. Proof of Theorem 3. Consider two arbitrary points $V_1^h, V_2^h \in \overline{S^h\left(R, P^h\right)}$. Let

(5.33)
$$W^h = V_2^h - V_1^h.$$

Then by (5.8), (5.18) and the triangle inequality

(5.34)
$$W^h \in S_0^h\left(2R\right) = \left\{V^h \in H_{N,0}^{1,h}\left(\Omega^h\right) : \left\|V^h\right\|_{H_N^{1,h}(\Omega^h)} \leq 2R\right\}.$$

Consider the vector function $F^h\left(V^h\left(\mathbf{x}^h\right),\mathbf{x}^h\right)$ in (5.12). It follows from (5.15), (5.33), Remark 5.1 and the multidimensional analog of the Taylor formula [49] that the following representation is valid

$$
\begin{aligned}
F\left(V_2^h\left(\mathbf{x}^h\right),\mathbf{x}^h\right) &= F\left(V_1^h\left(\mathbf{x}^h\right)+W^h\left(\mathbf{x}^h\right),\mathbf{x}^h\right) \\
&= F\left(V_1^h\left(\mathbf{x}^h\right),\mathbf{x}^h\right)+\widetilde{F}_1\left(V_1^h\left(\mathbf{x}^h\right),\mathbf{x}^h\right)W^h\left(\mathbf{x}^h\right) \\
&\quad +\widetilde{F}_2\left(V_1^h\left(\mathbf{x}^h\right),V_1^h\left(\mathbf{x}^h\right)+W^h\left(\mathbf{x}^h\right),\mathbf{x}^h\right),
\end{aligned}
$$
(5.35)

where $\widetilde{F}_1,\widetilde{F}_2$ are such that

(5.36)
$$
\left|\widetilde{F}_1\left(V_1^h\left(\mathbf{x}^h\right),\mathbf{x}^h\right)\right|\le C_1,
$$

(5.37)
$$
\left|\widetilde{F}_2\left(V_1^h\left(\mathbf{x}^h\right),V_1^h\left(\mathbf{x}^h\right)+W^h\left(\mathbf{x}^h\right),\mathbf{x}^h\right)\right|\le C_1\left(W^h\left(\mathbf{x}^h\right)\right)^2.
$$

In particular, (5.35) implies that the expression $\widetilde{F}_1\left(V_1^h\left(\mathbf{x}^h\right),\mathbf{x}^h\right)W^h\left(\mathbf{x}^h\right)$ is linear with respect to $W^h\left(\mathbf{x}^h\right)$. By (5.33), (5.35) and (5.37)

$$
\begin{aligned}
\left[L\left(V_1^h+W^h\right)+F\left(V_1^h\left(\mathbf{x}^h\right)+W^h\left(\mathbf{x}^h\right),\mathbf{x}^h\right)\right]^2 &= \\
= \left[\begin{array}{c} \left(L\left(V_1^h\right)+F\left(V_1^h\left(\mathbf{x}^h\right),\mathbf{x}^h\right)\right)+ \\ +\left(L\left(W^h\right)+\widetilde{F}_1\left(V_1^h\left(\mathbf{x}^h\right),\mathbf{x}^h\right)W^h\left(\mathbf{x}^h\right)\right)+ \\ +\widetilde{F}_2\left(V_1^h\left(\mathbf{x}^h\right),V_1^h\left(\mathbf{x}^h\right)+W^h\left(\mathbf{x}^h\right),\mathbf{x}^h\right) \end{array}\right]^2 &= \\
= \left[L\left(V_1^h\right)+F\left(V_1^h\left(\mathbf{x}^h\right),\mathbf{x}^h\right)\right]^2 + & \\
+2\left[L\left(V_1^h\right)+F\left(V_1^h\left(\mathbf{x}^h\right),\mathbf{x}^h\right)\right]\left[L\left(W^h\right)+\widetilde{F}_1\left(V_1^h\left(\mathbf{x}^h\right),\mathbf{x}^h\right)W^h\left(\mathbf{x}^h\right)\right] + & \\
+2\left[L\left(V_1^h\right)+F\left(V_1^h\left(\mathbf{x}^h\right),\mathbf{x}^h\right)\right]\left[\widetilde{F}_2\left(V_1^h\left(\mathbf{x}^h\right),V_1^h\left(\mathbf{x}^h\right)+W^h\left(\mathbf{x}^h\right),\mathbf{x}^h\right)\right] + & \\
+\left[\begin{array}{c} L\left(W^h\right)+\widetilde{F}_1\left(V_1^h\left(\mathbf{x}^h\right),\mathbf{x}^h\right)W^h\left(\mathbf{x}^h\right) \\ +\widetilde{F}_2\left(V_1^h\left(\mathbf{x}^h\right),V_1^h\left(\mathbf{x}^h\right)+W^h\left(\mathbf{x}^h\right),\mathbf{x}^h\right) \end{array}\right]^2 &
\end{aligned}
$$
(5.38)

Denote

(5.39)
$$
\begin{aligned}
I_{\mathrm{lin}}\left(V_1^h,W^h,\mathbf{x}^h\right) &= \\
= 2\left[L\left(V_1^h\right)+F\left(V_1^h\left(\mathbf{x}^h\right),\mathbf{x}^h\right)\right]\cdot\left[L\left(W^h\right)+\widetilde{F}_1\left(V_1^h\left(\mathbf{x}^h\right),\mathbf{x}^h\right)W^h\left(\mathbf{x}^h\right)\right], &
\end{aligned}
$$

(5.40)
$$
\begin{aligned}
I_{\mathrm{nonlin}}^{(1)}\left(V_1^h,W^h,\mathbf{x}^h\right) &= \\
= 2\left[L\left(V_1^h\right)+F\left(V_1^h\left(\mathbf{x}^h\right),\mathbf{x}^h\right)\right]\cdot\left[\widetilde{F}_2\left(V_1^h\left(\mathbf{x}^h\right),V_1^h\left(\mathbf{x}^h\right)+W^h\left(\mathbf{x}^h\right),\mathbf{x}^h\right)\right], &
\end{aligned}
$$

(5.41)
$$
\begin{aligned}
I_{\mathrm{nonlin}}^{(2)}\left(V_1^h,W^h,\mathbf{x}^h\right) &= \\
\left(L\left(W^h\right)+\widetilde{F}_1\left(V_1^h\left(\mathbf{x}^h\right),\mathbf{x}^h\right)W^h\left(\mathbf{x}^h\right)+\widetilde{F}_2\left(V_1^h\left(\mathbf{x}^h\right),V_1^h\left(\mathbf{x}^h\right)+W^h\left(\mathbf{x}^h\right),\mathbf{x}^h\right)\right)^2 &
\end{aligned}
$$

By (5.33) and (5.38)-(5.41)

$$
\begin{aligned}
(5.42) \quad & \left[L\left(V_2^h\right) + F\left(V_2^h\left(\mathbf{x}^h\right), \mathbf{x}^h\right)\right]^2 - \left[L\left(V_1^h\right) + F\left(V_1^h\left(\mathbf{x}^h\right), \mathbf{x}^h\right)\right]^2 = \\
& = I_{\mathrm{lin}}\left(V_1^h, W^h, \mathbf{x}^h\right) + I_{\mathrm{nonlin}}^{(1)}\left(V_1^h, W^h, \mathbf{x}^h\right) + I_{\mathrm{nonlin}}^{(2)}\left(V_1^h, W^h, \mathbf{x}^h\right).
\end{aligned}
$$

It follows from (5.37), (5.40) and (5.41) that

$$
\begin{aligned}
(5.43) \quad & \left|I_{\mathrm{nonlin}}^{(1)}\left(V_1^h, W^h, \mathbf{x}^h\right)\right| \le C_1 \left(W^h\left(\mathbf{x}^h\right)\right)^2, \ \forall W^h \in S_0^h\left(2R\right), \\
& \left|I_{\mathrm{nonlin}}^{(2)}\left(V_1^h, W^h, \mathbf{x}^h\right)\right| \le C_1 \left[\left(W_z^h\left(\mathbf{x}^h\right)\right)^2 + \left(W^h\left(\mathbf{x}^h\right)\right)^2\right], \ \forall W^h \in S_0^h\left(2R\right),
\end{aligned}
$$

where $S_0^h\left(2R\right)$ is defined in (5.34). By (5.17), (5.33) and (5.42)

$$
\begin{aligned}
(5.44) \quad & J_\lambda^h\left(V_2^h\right) - J_\lambda^h\left(V_1^h\right) = J_\lambda^h\left(V_1^h + W^h\right) - J_\lambda^h\left(V_1^h\right) = \\
& = \sum_{n=0}^{N-1} \sum_{(i,j)=(1,1)}^{(i,j)=(m-1,m-1)} \int_a^b I_{\mathrm{lin}}\left(V_1^h\left(x_i, y_j, z\right), W^h\left(x_i, y_j, z\right), x_i, y_j, z\right) e^{2\lambda z} dz \\
& + \sum_{n=0}^{N-1} \sum_{(i,j)=(1,1)}^{(i,j)=(m-1,m-1)} \int_a^b \sum_{k=1}^2 I_{\mathrm{nonlin}}^{(k)}\left(V_1^h\left(x_i, y_j, z\right), W^h\left(x_i, y_j, z\right), x_i, y_j, z\right) e^{2\lambda z} dz.
\end{aligned}
$$

Using (5.9), (5.43) and (5.44), we obtain

$$
\begin{aligned}
& \left|\sum_{n=0}^{N-1} \sum_{(i,j)=(1,1)}^{(i,j)=(m-1,m-1)} \int_a^b \sum_{k=1}^2 I_{\mathrm{nonlin}}^{(k)}\left(V_1^h\left(x_i, y_j, z\right), W^h\left(x_i, y_j, z\right), x_i, y_j, z\right) e^{2\lambda z} dz\right| \\
(5.45) \quad & \qquad\qquad \le C_1 e^{2\lambda b} \left\|W^h\right\|_{H_N^{1,h}\left(\Omega^h\right)}^2, \forall W^h \in S_0^h\left(2R\right).
\end{aligned}
$$

It follows from (5.39)-(5.41) that the expression in the second line of (5.44) is linear with respect to W^h. On the other hand, the expression in the third line of (5.44) is nonlinear with respect to W^h.

Consider the linear functional $J_{\lambda,\mathrm{lin}}^h\left(V_1^h\right)\left(W^h\right) : H_{N,0}^{1,h}\left(\Omega^h\right) \to \mathbb{R}$, which is the expression in the second line of (5.44). It follows from (5.7)-(5.10), (5.33), (5.36), (5.39) and (5.44) that

$$
\left|J_{\lambda,\mathrm{lin}}^h\left(V_1^h\right)\left(W^h\right)\right| \le C_1 e^{2\lambda b} \left\|W^h\right\|_{H_N^{1,h}\left(\Omega^h\right)}, \ \forall W^h \in H_N^{1,h}\left(\Omega^h\right).
$$

Hence, $J_{\lambda,\mathrm{lin}}^h\left(V_1^h\right)\left(W^h\right) : H_{N,0}^{1,h}\left(\Omega^h\right) \to \mathbb{R}$ is a bounded linear functional. By Riesz theorem there exists a vector function $\widetilde{J}_{\lambda,\mathrm{lin}}^h\left(V_1^h\right) \in H_{N,0}^{1,h}\left(\Omega^h\right)$ such that

$$
(5.46) \quad \left(\widetilde{J}_{\lambda,\mathrm{lin}}^h\left(V_1^h\right), Y^h\right) = J_{\lambda,\mathrm{lin}}^h\left(V_1^h\right)\left(Y^h\right), \forall Y^h \in H_{N,0}^{1,h}\left(\Omega^h\right).
$$

Also, using (5.43)-(5.46), we obtain

$$(5.47) \qquad \lim_{\|W^h\|_{H_N^{1,h}(\Omega^h)} \to 0} \frac{J_\lambda^h\left(V_1^h + W^h\right) - J_\lambda^h\left(V_1^h\right) - J_{\lambda,\text{lin}}^h\left(V_1^h\right)\left(W^h\right)}{\|W^h\|_{H_N^{1,h}(\Omega^h)}} = 0.$$

Hence, $J_{\lambda,\text{lin}}^h\left(V_1^h\right) : H_{N,0}^{1,h}\left(\Omega^h\right) \to \mathbb{R}$ is the Fréchet derivative of the functional $J_\lambda^h\left(V^h\right)$ at the point V_1^h. We denote it as

$$(5.48) \qquad \left(J_\lambda^h\right)'\left(V_1^h\right) := J_{\lambda,\text{lin}}^h\left(V_1^h\right).$$

The proof of the Lipschitz continuity property (5.20) of $\left(J_\lambda^h\right)'\left(V^h\right)$ is omitted here since it is completely similar with the proof of Theorem 3.1 of [2].

Using (5.36), (5.37), (5.41) and Cauchy-Schwarz inequality, we estimate now $I_{\text{nonlin}}^{(2)}(V_1^h, W^h, \mathbf{x}^h)$ from the below,

$$(5.49) \qquad I_{\text{nonlin}}^{(2)}\left(V_1^h, W^h, \mathbf{x}^h\right) \geq \frac{1}{2}\left(L\left(W^h\right)\right)^2 -$$

$$- \left[\widetilde{F}_1\left(V_1^h\left(\mathbf{x}^h\right), \mathbf{x}^h\right) W^h\left(\mathbf{x}^h\right) + \widetilde{F}_2\left(V_1^h\left(\mathbf{x}^h\right), V_1^h\left(\mathbf{x}^h\right) + W^h\left(\mathbf{x}^h\right), \mathbf{x}^h\right)\right]^2 \geq$$

$$\geq \frac{1}{2}\left(L\left(W^h\right)\right)^2 - C_1\left(W^h\left(\mathbf{x}^h\right)\right)^2.$$

Thus, Theorem 2, (5.44) and (5.48)-(5.49) imply

$$J_\lambda^h\left(V_1^h + W^h\right) - J_\lambda^h\left(V_1^h\right) - \left(J_\lambda^h\right)'\left(V_1^h\right)\left(W^h\right) \geq$$

$$(5.50) \qquad \geq \frac{1}{2}\left\|L\left(W^h\right)e^{\lambda z}\right\|_{L^{2,h}(\Omega^h)}^2 - C_1\left\|W^h e^{\lambda z}\right\|_{L^{2,h}(\Omega^h)}^2 \geq$$

$$\geq \frac{1}{4}\left\|\left(B_N W_z^h\right)e^{\lambda z}\right\|_{L_N^{2,h}(\Omega^h)}^2 + \frac{\lambda^2}{8}\left\|\left(B_N W^h\right)e^{\lambda z}\right\|_{L_N^{2,h}(\Omega^h)}^2 - C_1\left\|W^h e^{\lambda z}\right\|_{L^{2,h}(\Omega^h)}^2.$$

By Lemma 1 there exists a number $\widetilde{C}_1 = \widetilde{C}_1\left(B_N, N\right) > 0$ such that

$$\left\|\left(B_N W^h\right)e^{\lambda z}\right\|_{L_N^{2,h}(\Omega^h)}^2 \geq \widetilde{C}_1\left\|W^h e^{\lambda z}\right\|_{L_N^{2,h}(\Omega^h)}^2, \quad \forall W^h \in L^{2,h}\left(\Omega^h\right), \forall \lambda > 0,$$

and the same for $\left\|\left(B_N W_z^h\right)e^{\lambda z}\right\|_{L_N^{2,h}(\Omega^h)}^2$. Hence, (5.50) implies for all $\lambda \geq \lambda_0$

$$(5.51) \qquad J_\lambda^h\left(V_1^h + W^h\right) - J_\lambda^h\left(V_1^h\right) - \left(J_\lambda^h\right)'\left(V_1^h\right)\left(W^h\right)$$

$$\geq \widetilde{C}_1\left(\left\|W_z^h e^{\lambda z}\right\|_{L_N^{2,h}(\Omega^h)}^2 + \lambda^2\left\|W^h e^{\lambda z}\right\|_{L_N^{2,h}(\Omega^h)}^2\right) - C_1\left\|W^h e^{\lambda z}\right\|_{L^{2,h}(\Omega^h)}^2,$$

where $\lambda_0 \geq 1$ was chosen in Theorem 2. Choose the number $\lambda_1 \geq \lambda_0$ depending on the parameters listed in (5.21) such that $\widetilde{C}_1 \lambda_1^2/2 \geq C_1$ and keep in mind Remark 5.1. Then (5.51) implies (5.22). Given (5.22), the existence and uniqueness of the minimizer $V_{\min,\lambda}^h \in \overline{S^h\left(R, P^h\right)}$ of the functional $J_\lambda^h\left(V^h\right)$ on the set $\overline{S\left(R, P^h\right)}$ for every $\lambda \geq \lambda_1$ as well as inequality (5.23) follow immediately from a combination of Lemma 2.1 and Theorem 2.1 of [2]. $\square$

6. Numerical Studies.

6.1. Data simulation. We have conducted our numerical studies in the 2d case. Below $\mathbf{x} = (x, y)$, in (2.1) and (2.2) $a = 1, b = 2, A = 1/2$ and $d = 1/2$. Hence, we obtain

$$
\begin{aligned}
(6.1) \qquad &\Omega = \{\mathbf{x} : x \in (-1/2, 1/2), y \in (1, 2)\}, \\
&\Gamma_d = \{\mathbf{x}_\alpha = (\alpha, 0) : \alpha \in [-1/2, 1/2]\}, \qquad .
\end{aligned}
$$

In accordance with the conventional practice in the theory of inverse problems, we obtain the boundary data (2.18) via a computational simulation, i.e. via the numerical solution of the Forward Problem (2.15), (2.16). Following Theorem 1, we solve this problem via the solution of the integral equation (3.7). To solve this equation, we consider the partition of the intervals $(1, 2)$ and $(-1/2, 1/2)$ in (6.1) as:

$$
\begin{aligned}
(6.2) \qquad &1 = y_0 < y_1 < \cdots < y_{m_y} = 2, \quad y_{j+1} - y_j = h_y, \\
&\qquad h_y > 0, \quad j = 0, \cdots, m_y - 1, \\
&-1/2 = \alpha_0 < \alpha_1 < \cdots < \alpha_{m_\alpha} = 1/2, \quad \alpha_{j+1} - \alpha_j = h_\alpha, \\
&\qquad h_\alpha > 0, \quad j = 0, \cdots, m_\alpha - 1,
\end{aligned}
$$

where $m_y, m_\alpha > 1$ are two integers. Define the discrete subsets $(1, 2)_y^{h_y}$ and $(-1/2, 1/2)_\alpha^{h_\alpha}$ of the intervals $(1, 2)$ and $(-1/2, 1/2)$ as $(1, 2)_y^{h_y} = \{y_j\}_{j=0}^{m_y}$ and $(-1/2, 1/2)_\alpha^{h_\alpha} = \{\alpha_j\}_{j=0}^{m_\alpha}$. The fully discrete subset Ω_{discr}^h of the domain Ω is:

$$
\begin{aligned}
(6.3) \qquad &\Omega_{discr} = \{-1/2 = x_0 < x_1 < \cdots < x_m = 1/2\} \times (1, 2)_y^{h_y}, \\
&x_{j+1} - x_j = h, j = 0, \cdots, m - 1,
\end{aligned}
$$

see (5.1). Denote the corresponding sets of discrete points:

$$
(6.4) \qquad \mathbf{x}_{discr} = \left\{ (x_i, y_k) \in \Omega_{discr}^h \right\}, \quad \boldsymbol{\alpha}_{discr} = \left\{ (\alpha_i, 0, \cdots, 0) : \alpha_i \in (-1/2, 1/2)_\alpha^{h_\alpha} \right\}.
$$

To compute the numerical solution $u(\mathbf{x}_{discr}, \boldsymbol{\alpha}_{discr})$ of the Forward Problem (2.15), we need to perform the numerical integration in the integral equation (3.7). We note that the points in the integrals along the geodesic line $\Gamma(\mathbf{x}, \mathbf{x}_\alpha)$ do not necessary belong to the set Ω_{discr}. Hence, we describe now our numerical interpolation. For any point $(x^\Gamma, y^\Gamma) \in \Gamma(\mathbf{x}, \mathbf{x}_\alpha)$, we use the following formula of the numerical interpolation to approximate the value $U(x^\Gamma, y^\Gamma)$ of any function U involved in the numerical computation of the integral over $\Gamma(\mathbf{x}, \mathbf{x}_\alpha)$:

$$
\begin{aligned}
(6.5) \qquad U(x^\Gamma, y^\Gamma) \approx \frac{1}{h h_y} &\left(x_{j+1} - x^\Gamma \right) \left(y_{k+1} - y^\Gamma \right) U(x_j, y_k) \\
&+ \left(x_{j+1} - x^\Gamma \right) \left(y^\Gamma - y_k \right) U(x_j, y_{k+1}) \\
&+ \left(x^\Gamma - x_j \right) \left(y_{k+1} - y^\Gamma \right) U(x_{j+1}, y_k) \\
&+ \left(x^\Gamma - x_j \right) \left(y^\Gamma - y_k \right) U(x_{j+1}, y_{k+1})], \\
\text{for } &(x^\Gamma, y^\Gamma) \in [x_j, x_{j+1}] \times [y_k, y_{k+1}], \text{ see (6.2), (6.3).}
\end{aligned}
$$

As to the kernel $K(\mathbf{x}, \alpha, \beta)$ of the integral operator in (2.15), we work below with the 2D Henyey-Greenstein function [22]:

$$(6.6) \qquad K(\mathbf{x}, \alpha, \beta) = H(\alpha, \beta) = \frac{1}{2d} \left[\frac{1 - g^2}{1 + g^2 - 2g \cos(\alpha - \beta)} \right], \quad g = \frac{1}{2}.$$

Here, $g = 1/2$ means an anisotropic scattering, which is half ballistic with $g = 0$ an half isotropic scattering with $g = 1$ [13, 14, 15]. We take the same function $f(\mathbf{x})$ as the one in (2.3), (2.4) with $\epsilon = 0.05$.

6.2. Numerical results for the inverse problem. Just as in [34], we set

$$(6.7) \qquad \mu_s(\mathbf{x}) = 5, \ \mathbf{x} \in \Omega, \quad \mu_s(\mathbf{x}) = 0, \ \mathbf{x} \in \mathbb{R}^2 \setminus \Omega.$$

We use the third line of (2.12) for the coefficient function $a(\mathbf{x})$, and we take in this formula

$$(6.8) \qquad \mu_a(\mathbf{x}) = \begin{cases} c_a = const. > 0, & \text{inside the tested inclusion,} \\ 0, & \text{outside the tested inclusion.} \end{cases}$$

By (2.12), (6.7) and (6.8) we set:

$$(6.9) \qquad \text{correct inclusion/background contrast} = 1 + c_a/5,$$

$$(6.10) \qquad \begin{aligned} & \text{computed inclusion/background contrast} \\ & = 1 + \max \left(\text{computed } \mu_a(\mathbf{x}) \right) / 5. \end{aligned}$$

In all numerical tests below

$$(6.11) \qquad \varepsilon_r(\mathbf{x}) = \varepsilon_r(x, y) = \begin{cases} 1 + x^2 \ln(y) & y > 1, \\ 1 & \text{otherwise.} \end{cases}$$

This function $\varepsilon_r(x, y)$ satisfies conditions (2.7)-(2.9). Using the fast marching toolbox "Toolbox Fast Marching" [43] in MATLAB, we obtain the geodesic lines, and display examples on Figure 1.

The mesh sizes were chosen as $h_x = h_y = h_\alpha = h = 1/20$. Hence, we had total $20 \times 20 \times N$ unknown parameters in our minimization procedure. To solve the minimization problem, we have used the Matlab's built-in function **fminunc** with the quasi-newton algorithm. The iterations of the function **fminunc** were stopped at the iteration number k as soon as

$$\left| \nabla J_\lambda \left(V_k^h \right) \right| < 10^{-2}.$$

The random noise was introduced in the boundary data $g_1(\mathbf{x}, \alpha)$ in (4.12) as:

$$(6.12) \qquad g_1(\mathbf{x}, \alpha) = g_1(\mathbf{x}, \alpha) \left(1 + \delta \cdot \zeta_\mathbf{x} \right), \ \mathbf{x} \in \partial \Omega.$$

Here $\zeta_\mathbf{x}$ is the uniformly distributed random variable in the interval $[0, 1]$ depending on the point $\mathbf{x} \in \partial \Omega$ with $\delta = 0.03$ and $\delta = 0.05$, which correspond respectively to 3% and 5% noise level.
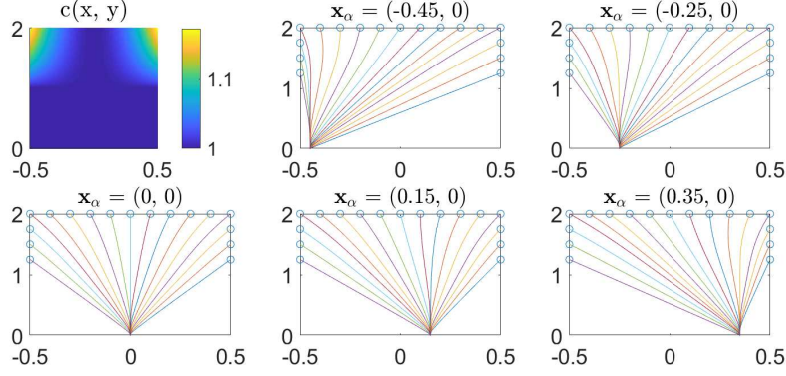
Figure 1: Samples of geodesic lines for the function $\varepsilon_r\left(\mathbf{x}\right)$, which is given in (6.11).

To solve the minimization problem, we need to provide the starting point $V_0^h(\mathbf{x}^h)$ for iterations. In all numerical tests below we choose the starting point as the discrete version of the following vector function $V_0(x,y) = \left(w_0^{(0)},...,w_{N-1}^{(0)}\right)^T(x,y)$:

(6.13)
$$w_n^{(0)}(x,y) = \frac{1}{2}\left(\frac{(A-x)}{2A}w_n(-A,y) + \frac{(x+A)}{2A}w_n(A,y)\right)$$
$$+ \frac{1}{2}\left(\frac{(b-y)}{b-a}w_n(x,a) + \frac{(y-a)}{b-a}w_n(x,b)\right), \quad n = 0,...,N-1.$$

Expression (6.13) represents the average of linear interpolations of the boundary condition for $w_n\left(x,y\right)$ inside of the square Ω with respect to $x-$direction and $y-$direction.

There are two parameters we need to choose: N and λ. We find the optimal pair $(N,\lambda) = (5,3)$ of these parameters in Test 1, see captions for Figures 2 and 3. Interestingly, the same optimal pair was found in [34] for a similar CIP for the regular RTE.

Remark 6.1. *To test the computational performance of the version of the convexification method of this paper, we have chosen letters-like shapes of abnormalities. This is because letters actually have complicated shapes for imaging via solutions of CIPs: they are non convex and have voids.*

We work with the noiseless data in Tests 1-3 and we work with the noisy data in Test 4.

Test 1. We test the letter 'A' with $c_a = 5$ in (6.8). We use this test to figure out optimal values of parameters N and λ.

First, we select an appropriate value of N. We use the value of the norms $\|w_n\left(\mathbf{x}\right)\|_{L_2(\Omega)}$ to indicate the information contained in $w_n\left(\mathbf{x}\right)$. Corresponding to the forward problem (2.15) and (2.16) for the case when the functions $\mu_s\left(\mathbf{x}\right)$ and $\mu_a\left(\mathbf{x}\right)$ are given in (6.7) and (6.8) respectively, and $c_a = 5$ in (6.8), we calculate norms $\|w_n\left(\mathbf{x}\right)\|_{L_2(\Omega)}$ for $n = 0,...,11$, and display them in Table 1. One can see that the $L_2\left(\Omega\right)-$norm of the function $w_n(\mathbf{x})$ decreases very rapidly when the number n is growing, and these norms, starting from $n = 3$ are much

less than those for $n = 0, 1, 2$. More precisely, we have obtained that

(6.14)
$$\frac{\sum\limits_{n=3}^{11} \|w_n(\mathbf{x})\|_{L_2(\Omega)}}{\sum\limits_{n=0}^{11} \|w_n(\mathbf{x})\|_{L_2(\Omega)}} = 0.0039,$$

which means 0.39%. We conclude therefore, that we should take in our tests $N = 3$.

Table 1: The $L_2(\Omega)-$norms of functions $w_n(\mathbf{x})$, $n = 0, 1, ..., 11$ for the reference Test 1 with $c_a = 5$ in (6.8).

n	0	1	2	3	4	5
$\|w_n(\mathbf{x})\|_{L_2}$	6.5365	1.8766	0.1924	0.0091	0.0071	0.0027
n	6	7	8	9	10	11
$\|w_n(\mathbf{x})\|_{L_2}$	0.0057	0.0020	0.0035	0.0012	0.0017	0.0008

Next, given the value of $N = 3$, we select the optimal value of the parameter λ of the Carleman Weight Function $e^{\lambda z}$ in (5.17). To do this, we test the same letter 'A' with $c_a = 5$ inside of it for values of the parameter $\lambda = 0, 1, 2, 3, 4, 5, 6, 8, 20$. Our numerical results are presented on Figure 2. We observe that the images have a low quality for $\lambda = 0, 1$. Then the quality is improved, and it is stabilized at $\lambda = 5$. Hence, we treat $\lambda = 5$ as the optimal value of this parameter. Thus, we use in all our tests below

$$N = 3, \lambda = 5.$$

At last, we want to demonstrate numerically again that $N = 3$ is indeed a good choice of N for our optimal value of $\lambda = 5$. Taking $\lambda = 5$, we test the same letter 'A' as above with $c_a = 5$ in it, but for $N = 1, 2, 3, 5, 7, 12$. The results are displayed in Figure 3. One can observe that reconstructions have a low quality for $N = 1, 2$. Next, the reconstructions are basically the same for $N = 3, 5, 7, 12$. However, the computational cost increases very rapidly with the increase of N. Thus, we conclude that to balance between the reconstruction accuracy and the computational cost, we should use $N = 3$, which coincides with the above choice.

Test 2. We test the reconstruction of the coefficient $a(\mathbf{x})$ with the shape of the letter 'A' where the function $\mu_a(\mathbf{x})$ is given in (6.8). We test different values of the parameter $c_a = 10, 15, 20, 30$ inside of the letter 'A'. Thus, by (6.9) the inclusion/background contrasts now are respectively $3 : 1$, $4 : 1$, $5 : 1$ and $6 : 1$. The function $\varepsilon_r(\mathbf{x}) = \varepsilon_r^{(1)}(\mathbf{x})$ as in (6.11). Our computational results for this test are displayed on Figure 4. One can observe that the quality of these images is good for all four cases, although it slightly deteriorates for $c_a = 20$ and $c_a = 30$. The computed inclusion/background contrast is accurate, see (6.10) and compare with (6.9).

Test 3. We test the reconstruction of the coefficient $a(\mathbf{x})$ with the shape of two letters 'SZ', where the function $\mu_a(\mathbf{x})$ is given in (6.8) with $c_a = 5$ inside of each of these two letters, and $\mu_a(\mathbf{x}) = 0$ outside of each of these two letters. SZ are two letters in the name of the city
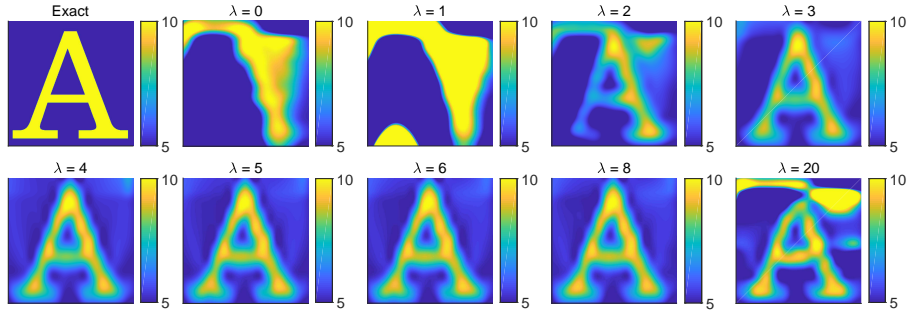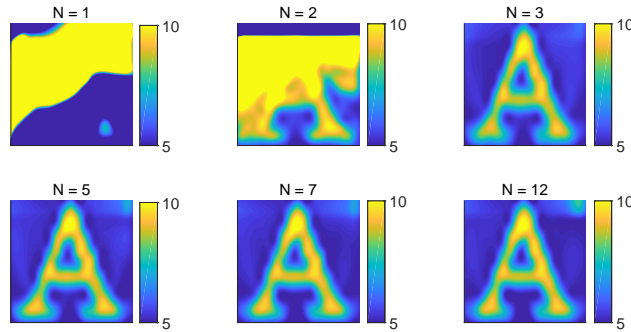
Figure 2: Test 1. The reconstructed coefficient $a(\mathbf{x})$, where the function $\mu_a(\mathbf{x})$ is given in (6.8) with $c_a = 5$ inside of the letter 'A'. The goal here is to test different values of the parameter $\lambda = 0, 1, 2, 3, 4, 5, 6, 8, 20$ for $N = 3$. The value of λ can be seen on the top side of each square. The images have a low quality for $\lambda = 0, 1, 2, 3$. Then the quality is improved and is stabilized at $\lambda = 5$. Thus, we select $\lambda = 5$ as an optimal value of this parameter for all follow up tests. On the other hand, the last image is for the case $\lambda = 20$. This image demonstrates that the quality of the reconstructions deteriorates for too large value of λ.

Figure 3: Test 1. The reconstructed coefficient $a(\mathbf{x})$, where the function $\mu_a(\mathbf{x})$ is given in (6.8) with $c_a = 5$ inside of the letter 'A'. We took the optimal value of the parameter $\lambda = 5$ (see Figure 2) and have tested different values of the parameter $N = 1, 2, 3, 5, 7, 12$. A low quality can be observed for $N = 1, 2$. The reconstructions are basically the same for $N = 3, 5, 7, 12$. However, the computational cost increases very rapidly with the increase of N. We conclude, therefore, that to balance between the reconstruction accuracy and the computational cost, we should use $N = 3$. Thus, we use below $\lambda = 5$ and $N = 3$.

(Shenzhen) were the second and the fifth authors reside. The results are displayed on Figure 5.

Test 4. We now use the noisy data as in (6.12) with $\delta = 0.03$ and $\delta = 0.05$, i.e. with 3% and 5% noise level. We test the reconstruction of the coefficient $a(\mathbf{x})$ with the shape of either the letter 'A' or the letter 'Ω', where the function $\mu_a(\mathbf{x})$ is given in (6.8) with $c_a = 5$
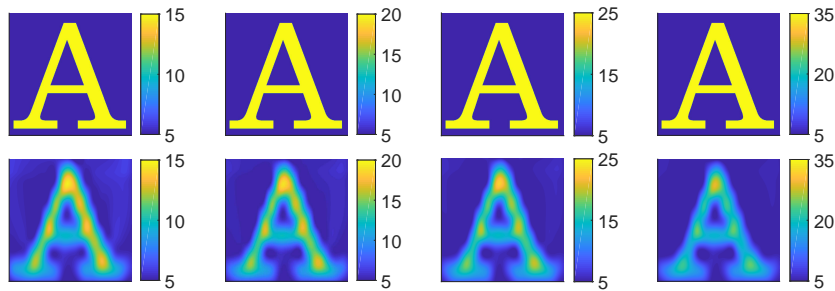
Figure 4: Test 2. Exact (top) and reconstructed (bottom) coefficient $a(\mathbf{x})$ for $c_a = 10, 15, 20, 30$ (from left to right) inside of the letter 'A' as in (6.8). Thus, by (6.9) the inclusion/background contrasts now are respectively $3:1$, $4:1$, $5:1$ and $6:1$. The image quality remains basically the same for all these values of the parameter c_a, although a slight deterioration of this quality can be observed for $c_a = 20$ and $c_a = 30$. The computed inclusion/background contrasts (6.9) are reconstructed accurately.
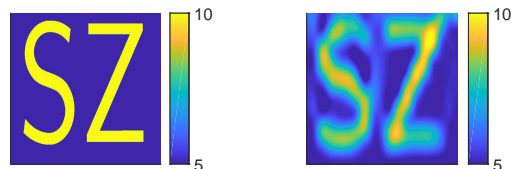

Figure 5: Test 3. Exact (left) and reconstructed (right) coefficient $a(\mathbf{x})$ for the case when the function $\mu_a(\mathbf{x})$ is given in (6.8) with $c_a = 5$ with the shape of two letters 'SZ'. In (6.8) $c_a = 5$ inside of each of these two letters and $\mu_a(\mathbf{x}) = 0$ outside of each of these two letters. Here $N = 3, \lambda = 5$. The quality is good and the computed inclusion/background contrasts are accurately reconstructed in both letters, see (6.9) and (6.10).

inside of each of these two letters. The results are displayed on Figure 6. One can observe accurate reconstructions in all four cases. In particular, the inclusion/background contrasts are reconstructed accurately, see (6.10) and compare with (6.9).

REFERENCES

[1] M. ASADZADEH AND L. BEILINA, *A stabilized P1 domain decomposition finite element method for time harmonic Maxwell's equations*, Math. Comput. Simul, 204 (2023), pp. 556–574.

[2] A. B. BAKUSHINSKII, M. V. KLIBANOV, AND N. A. KOSHEV, *Carleman weight functions for a globally convergent numerical method for ill-posed Cauchy problems for some quasilinear PDEs*, Nonlinear Anal. Real World Appl., 34 (2017), pp. 201–224.

[3] G. BAL, *Inverse transport theory and applications*, Inverse Probl., 25 (2009), p. 053001.

[4] G. BAL AND A. JOLLIVET, *Generalized stability estimates in inverse transport theory*, Inverse Probl. Imaging, 12 (2018), pp. 59–90.

[5] G. BAL AND A. TAMASAN, *Inverse source problems in transport equations*, SIAM J. Math. Anal., 39 (2007), pp. 57–76.
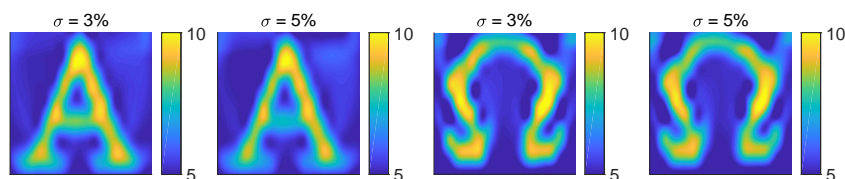
Figure 6: Test 4. Reconstructed coefficient $a(\mathbf{x})$ with the shape of letters 'A' and 'Ω' with $c_a = 5$ from noise polluted observation data as in (6.12) with $\delta = 0.03$ and $\delta = 0.05$, i.e. with 3% and 5% noise level. One can observe accurate reconstructions in all four cases. In particular, the inclusion/background contrasts are reconstructed accurately, see (6.9) and (6.10).

[6] L. BEILINA, M. G. ARAM, AND E. M. KARCHEVSKII, *An adaptive finite element method for solving 3D electromagnetic volume integral equation with applications in microwave thermometry*, J. Comput. Phys., 459 (2022), p. 111122.

[7] L. BEILINA AND E. LINDSTROM, *An adaptive finite element/finite difference domain decomposition method for applications in microwave imaging*, Electronics, 11 (2022), p. 1359.

[8] M. BELLASSOUED AND M. YAMAMOTO, *Carleman estimates and applications to inverse problems for hyperbolic systems*, Springer, Japan, 2017.

[9] M. BORN AND E. WOLF, *Principles of optics*, Cambridge University Press, 7th ed., 1999.

[10] A. L. BUKHGEIM AND M. V. KLIBANOV, *Uniqueness in the large of a class of multidimensional inverse problems*, Soviet Math. Doklady, 17 (1981), pp. 244–247.

[11] M. CRISTOFOL, S. LI, AND Y. SHANG, *Carleman estimates and some inverse problems for the coupled quantitative thermoacoustic equations by partial boundary layer data. Part II: Some inverse problems*, Math. Methods Appl. Sci., published online, (2023), https://doi.org/10.1002/mma.9252.

[12] S.-R. FU AND P.-F. YAO, *Stability in inverse problem of an elastic plate with a curved middle surface*, Inverse Probl., 39 (2023), p. 045003.

[13] H. FUJIWARA, K. SADIQ, AND A. TAMASAN, *A Fourier approach to the inverse source problem in an absorbing and anisotropic scattering medium*, Inverse Probl., 36 (2020), p. 015005.

[14] H. FUJIWARA, K. SADIQ, AND A. TAMASAN, *Numerical reconstruction of radiative sources in an absorbing and nondiffusing scattering medium in two dimensions*, SIAM J. Imaging Sci., 13 (2020), pp. 535–555.

[15] H. FUJIWARA, K. SADIQ, AND A. TAMASAN, *A source reconstrution method in two dimensional radiative transport using boundary data measured on an arc*, Inverse Probl., 37 (2021), p. 115005.

[16] G. GIORGI, M. BRIGNONE, R. ARAMINI, AND M. PIANA, *Application of the inhomogeneous Lippmann–Schwinger equation to inverse scattering problems*, SIAM J. Appl. Math., 73 (2013), pp. 212–231.

[17] F. GÖLGELEYEN AND M. YAMAMOTO, *Stability for some inverse problems for transport equations*, SIAM J. Math. Anal., 48 (2016), pp. 2319–2344.

[18] A. V. GONCHARSKY AND S. Y. ROMANOV, *Iterative methods for solving coefficient inverse problems of wave tomography in models with attenuation*, Inverse Probl., 33 (2017), p. 025003.

[19] A. V. GONCHARSKY AND S. Y. ROMANOV, *A method of solving the coefficient inverse problems of wave tomography*, Comput. Math. Appl., 77 (2019), pp. 967–980.

[20] J. P. GUILLEMENT AND R. G. NOVIKOV, *Inversion of weighted Radon transforms via finite Fourier series weight approximation*, Inverse Probl. Sci. En., 22 (2013), pp. 787–802.

[21] E. HASSI, S.-E. CHORFI, AND L. MANIAR, *Stable determination of coefficients in semilinear parabolic system with dynamic boundary conditions*, Inverse Probl., 38 (2022), p. 115007.

[22] J. HEINO, S. ARRIDGE, J. SIKORA, AND E. SOMERSALO, *Anisotropic effects in highly scattering media*, Phys. Rev. E, 68 (2003), p. 03198.

[23] V. ISAKOV, *Inverse Problems for Partial Differential Equations*, Springer, New York, 2006.

[24] S. I. KABANIKHIN, N. S. NOVIKOV, I. V. OSELEDETS, AND M. A. SHISHLENIN, *Fast toeplitz linear system*

inversion for solving two-dimensional acoustic inverse problem, J. Inverse Ill-Posed Probl., 23 (2015), pp. 687–700.

[25] S. I. KABANIKHIN, K. K. SABELFELD, N. S. NOVIKOV, AND M. A. SHISHLENIN, *Numerical solution of an inverse problem of coefficient recovering for a wave equation by a stochastic projection methods*, Monte Carlo Methods Appl., 21 (2015), pp. 189–203.

[26] V. A. KHOA, M. V. KLIBANOV, AND L. H. NGUYEN, *Convexification for a 3D inverse scattering problem with the moving point source*, SIAM J. Imag. Sci., 13 (2020), pp. 871–904.

[27] M. KLIBANOV AND M. YAMAMOTO, *Exact controllability for the time dependent transport equation*, SIAM J. Control Optim., 46 (2007), pp. 2071–2195.

[28] M. V. KLIBANOV, *Inverse problems and Carleman estimates*, Inverse Probl., 8 (1992), pp. 575–596.

[29] M. V. KLIBANOV, *Global convexity in a three-dimensional inverse acoustic problem*, SIAM J. Math. Anal., 28 (1997), pp. 1371–1388.

[30] M. V. KLIBANOV, *Carleman estimates for global uniqueness, stability and numerical methods for coefficient inverse problems*, J. Inverse Ill-Posed Probl., 21 (2013), pp. 477–510.

[31] M. V. KLIBANOV, *Convexification of restricted Dirichlet to Neumann map*, J. Inverse Ill-Posed Probl., 25 (2017), pp. 669–685.

[32] M. V. KLIBANOV AND O. V. IOUSSOUPOVA, *Uniform strict convexity of a cost functional for three-dimensional inverse scattering problem*, SIAM J. Math. Anal, 26 (1995), pp. 147–179.

[33] M. V. KLIBANOV AND J. LI, *Inverse Problems and Carleman Estimates: Global Uniqueness, Global Convergence and Experimental Data*, De Gruyter, 2021.

[34] M. V. KLIBANOV, J. LI, L. NGUYEN, AND Z. YANG, *Convexification numerical method for a coefficient inverse problem for the radiative transport equation*, SIAM J. Imag. Sci., 16 (2023), pp. 35–63, https://doi.org/10.1137/22m1509837.

[35] M. V. KLIBANOV, J. LI, AND Z. YANG, *Convexification for the viscosity solution for a coefficient inverse problem for the radiative transfer equation*, arXiv:2302.12474, (2023).

[36] M. V. KLIBANOV AND S. PAMYATNYKH, *Global uniqueness for a coefficient inverse problem for the non-stationary transport equation via Carleman estimate*, J. Math. Anal. Appl., 343 (2008), pp. 352–365.

[37] M. V. KLIBANOV AND V. G. ROMANOV, *A hölder stability estimate for a coefficient inverse problem for the wave equation with a point source*, Eurasian J. Math. Comp., 10(2) (2022), pp. 11–25.

[38] R. Y. LAY AND Q. LI, *Parameter reconstruction for general transport equation*, SIAM J. Math. Anal., 52 (2020), pp. 2734–2758.

[39] J. LI, H. LIU, AND S. MA, *Determining a random schrö dinger operator: both potential and source are random*, Commun. Math. Phys., 381 (2021), pp. 527–556.

[40] J. LI, H. LIU, L. RONDI, AND U. G., *Regularized Transformation-Optics Cloaking for the Helmholtz Equation: From Partial Cloak to Full Cloak*, Commun. Math. Phys., 335(2) (2015), pp. 671–712.

[41] S. R. MCDOWALL, *An inverse problem for the transport equation in the presence of a Riemannian metric*, Pac. J. Math., 216 (2004), pp. 303–326.

[42] R. NOVIKOV AND M. SANTACESARIA, *Monochromatic reconstruction algorithms for two-dimensional multi-channel inverse problems*, Int. Math. Res. Not., 2013 (2012), pp. 1205–1229.

[43] G. PEYRE, *Toolbox fast marching*, MATLAB Central File Exchange, (2023).

[44] V. G. ROMANOV, *Inverse Problems of Mathematical Physics*, VNU Press, Utrecht, The Netherlands, 1986.

[45] V. G. ROMANOV, *Inverse problems for differential equations with memory*, Eurasian J. Math. Comp., 2 (2014), pp. 51–80.

[46] J. A. SCALES, M. L. SMITH, AND T. L. FISCHER, *Global optimization methods for multimodal inverse problems*, J. Comp. Phys., 103 (1992), pp. 258–268.

[47] A. V. SMIRNOV, M. V. KLIBANOV, AND L. H. NGUYEN, *On an inverse source problem for the full radiative transfer equation with incomplete data*, SIAM J. Sci. Comput., 41 (2019), pp. B929–B952.

[48] A. N. TIKHONOV, A. V. GONCHARSKY, V. V. STEPANOV, AND A. G. YAGOLA, *Numerical methods for the solution of ill-posed problems*, Kluwer, London, 1995.

[49] M. M. VAJNBERG, *Variational method and method of monotone operators in the theory of nonlinear equations*, Israel Program for Scientific Translations, Jerusalem-London, 1973.

[50] M. YAMAMOTO, *Carleman estimates for parabolic equations*, Topical Review. Inverse Probl., 25 (2009), p. 123013.